

GEOLOGICAL SURVEY CIRCULAR 795



Estimation of Ground Motion Parameters

Estimation of Ground Motion Parameters

By David M. Boore, William B. Joyner,
Adolph A. Oliver III, and Robert A. Page

GEOLOGICAL SURVEY CIRCULAR 795

Prepared on behalf of the Nuclear Regulatory Commission

United States Department of the Interior

CECIL D. ANDRUS, *Secretary*



Geological Survey

H. William Menard, *Director*

CONTENTS

	Page
Abstract-----	1
Introduction-----	1
Data characteristics and methods of presentation-----	1
All earthquakes-----	5
San Fernando earthquake-----	17
Previously published curves for peak acceleration-----	23
Estimation of peak parameters at short distances-----	25
References cited-----	26
Statistical parameters-----	30
Strong-motion data-----	32

TABLE

Table 1. Sources of data used in assigning magnitudes and station distances-----	2
--	---

ILLUSTRATIONS

Figure 1-48. Graphs showing:

1. Peak horizontal acceleration versus distance to slipped fault for magnitude range 5.0-5.7-----	6
2. Peak horizontal acceleration versus distance to slipped fault for magnitude range 6.0-6.4-----	7
3. Peak horizontal acceleration versus distance to slipped fault for magnitude range 7.1-7.6-----	7
4. Comparison of 70 percent prediction intervals for peak horizontal acceleration for all three magnitude classes-----	7
5. Peak horizontal velocity versus distance to slipped fault for magnitude range 5.3-5.7-----	8
6. Peak horizontal velocity versus distance to slipped fault for magnitude 6.4-----	8
7. Peak horizontal velocity versus distance to slipped fault for magnitude range 7.1-7.2-----	8
8. Comparison of 70 percent prediction intervals for peak horizontal velocity for three magnitude classes-----	9
9. Peak horizontal displacement versus distance to slipped fault for magnitude range 5.3-5.7-----	9
10. Peak horizontal displacement versus distance to slipped fault for magnitude 6.4-----	9
11. Peak horizontal displacement versus distance to slipped fault for magnitude range 7.1-7.2-----	10
12. Comparison of 70 percent prediction intervals for peak horizontal displacement for three magnitude classes-----	10
13. Duration versus distance from slipped fault for recordings from small structures.-----	10
14. Peak vertical acceleration versus distance to slipped fault for magnitude range 5.0-5.7-----	11
15. Peak vertical acceleration versus distance to slipped fault for magnitude range 6.0-6.4-----	11

ILLUSTRATIONS, CONTINUED

	Page
16. Peak vertical acceleration versus distance to slipped fault for magnitude range 7.1-7.6-----	11
17. Peak vertical velocity versus distance to slipped fault for magnitude range 5.3-5.7-----	12
18. Peak vertical velocity versus distance to slipped fault for magnitude 6.4-----	12
19. Peak vertical velocity versus distance to slipped fault for magnitude range 7.1-7.2-----	12
20. Peak vertical displacement versus distance to slipped fault for magnitude range 5.3-5.7-----	13
21. Peak vertical displacement versus distance to slipped fault for magnitude 6.4-----	13
22. Peak vertical displacement versus distance to slipped fault for magnitude range 7.1-7.2-----	13
23. Peak horizontal acceleration versus distance to slipped fault for magnitude range 5.0-5.7 including data from both large and small structures-----	14
24. Peak horizontal acceleration versus distance to slipped fault for magnitude range 6.0-6.4 including data from both large and small structures-----	14
25. Peak horizontal acceleration versus distance to slipped fault for magnitude range 7.1-7.6 including data from both large and small structures-----	14
26. Peak horizontal velocity versus distance to slipped fault for magnitude range 5.3-5.7 including data from both large and small structures-----	15
27. Peak horizontal velocity versus distance to slipped fault for magnitude 6.4 including data from both large and small structures-----	15
28. Peak horizontal velocity versus distance to slipped fault for magnitude range 7.1-7.2 including data from both large and small structures-----	15
29. Peak horizontal displacement versus distance to slipped fault for magnitude range 5.3-5.7 including data from both large and small structures-----	16
30. Peak horizontal displacement versus distance to slipped fault for magnitude 6.4 including data from both large and small structures-----	16
31. Peak horizontal displacement versus distance to slipped fault for magnitude range 7.1-7.2 including data from both large and small structures-----	16
32. Peak horizontal acceleration versus distance to slipped fault at soil sites, San Fernando earthquake-----	18
33. Comparison of mean regression lines and 70 percent prediction intervals for large and small structures for peak horizontal acceleration at soil sites, San Fernando earthquake-----	18
34. Peak horizontal velocity versus distance to slipped fault at soil sites, San Fernando earthquake-----	19

ILLUSTRATIONS, CONTINUED

	Page
35. Comparison of mean regression lines and 70 percent prediction intervals for large and small structures for peak horizontal velocity at soil sites, San Fernando earthquake-----	19
36. Peak horizontal displacement versus distance to slipped fault at soil sites, San Fernando earthquake-----	19
37. Comparison of mean regression lines and 70 percent prediction intervals for large and small structures for peak horizontal displacement at soil sites, San Fernando earthquake-----	20
38. Peak horizontal acceleration recorded at base of small structures versus distance to slipped fault, San Fernando earthquake-----	20
39. Comparison of mean regression lines and 70 percent prediction intervals for rock and soil sites for peak horizontal acceleration recorded at base of small structures, San Fernando earthquake-----	20
40. Peak horizontal velocity recorded at base of small structures versus distance to slipped fault, San Fernando earthquake-----	21
41. Comparison of mean regression lines and 70 percent prediction intervals for rock and soil sites for peak horizontal velocity recorded at base of small structures, San Fernando earthquake-----	21
42. Peak horizontal displacement recorded at base of small structures versus distance to slipped fault, San Fernando earthquake-----	21
43. Comparison of mean regression lines and 70 percent prediction intervals for rock and soil sites for peak horizontal displacement recorded at base of small structures, San Fernando earthquake-----	22
44. Azimuthal dependence of peak horizontal acceleration recorded at base of small structures, San Fernando earthquake-----	22
45. Azimuthal dependence of peak horizontal velocity recorded at base of small structures, San Fernando earthquake-----	22
46. Azimuthal dependence of peak horizontal displacement recorded at base of small structures, San Fernando earthquake-----	23
47. Proposed relations of peak horizontal acceleration to distance from slipped fault for magnitude 6.6 earthquake-----	24
48. Proposed relations of peak horizontal acceleration to distance from slipped fault for magnitude 7.6 earthquake-----	24

Estimation of Ground Motion Parameters

By David M. Boore, William B. Joyner, Adolph A. Oliver III, and Robert A. Page

ABSTRACT

Strong motion data from western North America for earthquakes of magnitude greater than 5 are examined to provide the basis for estimating peak acceleration, velocity, displacement, and duration as a function of distance for three magnitude classes. A subset of the data (from the San Fernando earthquake) is used to assess the effects of structural size and of geologic site conditions on peak motions recorded at the base of structures. Small but statistically significant differences are observed in peak values of horizontal acceleration, velocity and displacement recorded on soil at the base of small structures compared with values recorded at the base of large structures. The peak acceleration tends to be less and the peak velocity and displacement tend to be greater on the average at the base of large structures than at the base of small structures. In the distance range used in the regression analysis (15-100 km) the values of peak horizontal acceleration recorded at soil sites in the San Fernando earthquake are not significantly different from the values recorded at rock sites, but values of peak horizontal velocity and displacement are significantly greater at soil sites than at rock sites.

Some consideration is given to the prediction of ground motions at close distances where there are insufficient recorded data points. As might be expected from the lack of data, published relations for predicting peak horizontal acceleration give widely divergent estimates at close distances (three well known relations predict accelerations between $0.33g$ to slightly over $1g$ at a distance of 5 km from a magnitude 6.5 earthquake). After considering the physics of the faulting process, the few available data close to faults, and the modifying effects of surface topography, at the present time it would be difficult to accept estimates less than about $0.8g$, 110 cm/s, and 40 cm, respectively, for the mean values of peak acceleration, velocity, and displacement at rock sites within 5 km of fault rupture in a magnitude 6.5 earthquake. These estimates can be expected to change as more data become available.

INTRODUCTION

Peak horizontal acceleration is commonly used to scale response spectra or ground motion time histories for use in earthquake resistant design, particularly for nuclear power plant facilities (Newmark, Blume, and Kapur, 1973). Methods have also been proposed (Newmark and Hall, 1969) for constructing design spectra using three peak parameters --horizontal acceleration, velocity, and displacement--the advantage of using all three parameters being that together they convey some information concerning the shape of the spectrum as well as the amplitude level. In this report we present the analysis of a large number of earthquake data to provide the basis for estimating the peak acceleration, velocity, and displacement and duration of shaking for a hypothetical earthquake of a prescribed magnitude at a prescribed distance from the causative fault. This work is a continuation of that reported by Page, Boore, Joyner, and Coulter (1972) and by Page, Boore, and Dieterich (1975).

It is not our purpose to advocate the use of peak parameters in scaling design motions. We look forward ultimately to the development of new methods for prescribing design motions, methods more firmly based in the physics that governs faulting and wave propagation. Pending the development of such methods, we recognize widespread current practice and attempt to present the available strong motion data in a compact and useful form for estimating peak parameters.

Acknowledgments. -- We are grateful to R. P. Maley for assistance in obtaining information on strong-motion recording site conditions and to A. G. Brady for unpublished strong motion data.

DATA CHARACTERISTICS AND METHODS OF PRESENTATION

Sources of data. -- The data set includes 204 recordings from 19 earthquakes and is listed in the table of "strong motion data" (end of report). The primary source of acceleration data is volume I of the series "Strong-Motion Earthquake Accelerograms" published under the direction of D. E. Hudson by the Earthquake Engineering Research Laboratory of the California Institute of Technology; values of

velocity, displacement, and duration came from volume II of the same series. We used volume I for acceleration because volume II gives data at equal time intervals of 0.02 s, which tends to bias the peak acceleration toward lower values. A few of the acceleration data came from other sources listed in the table of "strong-motion data", principally *U.S. Earthquakes*, an annual publication of the U. S. Department of Commerce.

Distances. -- In all cases the distance used is the shortest distance between the surface of fault slippage and the recording point. This would clearly be the preferred measure of distance if radiation were uniform over the surface and if the surface were known. The second condition is sometimes not met; the first is probably never met. Other measures of distance have been used in strong motion data analysis, particularly epicentral distance, hypocentral distance, and distance from the center of energy release. The use of epicentral distance or hypocentral distance has the advantage that these measures are more commonly known and special studies are not required to determine them. In some cases, however, these measures are clearly inappropriate, as for a long fault rupture with the epicenter at one end and recording stations at the other. The Parkfield, California, earthquake of 1966 provides an example of such a situation. The use of

distance to the center of energy release is a way of avoiding the assumption of uniform radiation over the rupture surface, but for long ruptures this measure, too, may be inappropriate. In our opinion the best choice for general purposes is the closest distance to the rupture surface, but the uncertainties resulting from nonuniform radiation over the surface should be kept in mind. An illustration of those uncertainties, is provided by the Pacoima Dam recording of the San Fernando earthquake of 1971. On that record the source for peak velocity and for the peak acceleration are different points on the fault, separated by perhaps 20 km, neither one of which is the closest point to the instrument (Hanks, 1974; Bouchon and Aki, 1977).

With a few exceptions the location of the rupture surface has been inferred from the aftershock distribution. For the Imperial Valley, California, earthquake of 1940 the distance used is chosen in accordance with the interpretations of Richter (1958) and Trifunac and Brune (1970). For the Hebgen Lake, Montana, earthquake of 1959, the distance used is the epicentral distance of the main shock, and for the Puget Sound earthquake of 1949, the distance used is the hypocentral distance of the main shock, assuming a minimum focal depth of 45 km. Sources of data used in estimating station distances are included in table I.

Table I.--Sources of data used in assigning magnitudes and station distances

Earthquake	Date (GMT)			Sources
	Month	Day	Year	
Imperial Valley, California-----	5	19	40	Trifunac and Brune (1970); Trifunac (1972); Richter (1958).
Puget Sound, Washington-----	4	13	49	Nuttli (1952); Page, Boore, Joyner, and Coulter (1972).
Kern County, California-----	7	21	52	Richter (1958); Page, Boore, Joyner, and Coulter (1972); Bolt (1978).
Daly City, California-----	3	22	57	Tocher (1959); Cloud (1959).
Hebgen Lake, Montana-----	8	18	59	Tocher (1962); Page, Boore, Joyner, and Coulter (1972).
Parkfield, California-----	6	28	66	McEvelly and others (1967); Lindh and Boore (1973); Trifunac and Udawadia (1974); A. G. Lindh (oral commun., 1976).
Fairbanks, Alaska-----	6	21	67	Gedney and Berg (1969).

Table 1.--Sources of data used in assigning magnitudes and station distances--Continued

Earthquake	Date (GMT)			Sources
	Month	Day	Year	
Borrego Mountain, California----	4	9	68	Allen and Nordquist (1972); Hamilton (1972).
Santa Rosa, California-----	10	2	69	Steinbrugge and others (1970); Unger and Eaton (1970); J. D. Unger and J. P. Eaton (written commun., 1976).
Lytle Creek, California-----	9	12	70	T. C. Hanks (written commun., 1971).
San Fernando, California-----	2	9	71	Allen, Hanks and Whitcomb (1973); Allen and others (1971); R. L. Wesson (written commun., 1974).
Bear Valley, California-----	2	24	72	Ellsworth (1975).
Sitka, Alaska-----	7	30	72	Page and Gawthrop (1973); W. H. Gawthrop and R. A. Page (unpub. data).
Managua, Nicaragua-----	12	23	72	Dewey and others (1973); Ward and others (1973); Knudson and Hansen, A. (1973).
Point Mugu, California-----	2	21	73	Ellsworth and others (1973); Boore and Stierman (1976); Stierman and Ellsworth (1976).
Bear Valley, California-----	11	28	74	Person (1975); W. H. K. Lee (written commun., 1976).
Oroville, California-----	1	8	75	Bufe and others (1976); Lahr and others (1976).
Ferndale, California-----	6	7	75	Nason and others (1975); Stewart Smith (written commun., 1976).

In order to avoid obscuring the attenuation relation, we generally exclude data where the uncertainty in distance is large. Following Page, Boore, Joyner, and Coulter (1972), we classify the distances as A, B, or C, according to the uncertainty (less than 2 km, 2 to 5 km, and 5 to 25 km, respectively). C quality data are only used for the magnitude 7.1 Puget Sound earthquake and the magnitude 7.1 Hebgen Lake earthquake. In the plots to follow, the class A, B, or C is indicated by the size of the symbol, the largest for class A and the smallest for class C.

The assignment of distances for the Parkfield earthquake deserves special mention. Originally it was believed that the

rupture associated with the Parkfield earthquake extended along the San Andreas fault far enough to the southeast so that it passed within 80 meters of station 2 of the Cholame-Shandon array (Cloud and Perez, 1967). Lindh and Boore (1973), however, presented evidence that, at the time of the earthquake, no significant displacement occurred beyond a point 7 km northwest of station 2. Modeling studies by Trifunac and Udvardia (1974) tend to confirm the interpretation of Lindh and Boore and we follow it in this report.

Classification of data. -- We have divided the data into classes in accordance with magnitude, site geology, and size of associated structure. The data were divided

into three magnitude classes (5.0-5.7, 6.0-6.4, and 7.1-7.6) on the basis of the Richter local magnitude (Richter, 1958), if available; otherwise surface wave magnitude is used. Sources of data for assigning magnitudes are included in table I. The Imperial Valley earthquake is assigned a magnitude of 6.4 in accordance with a determination by Trifunac and Brune (1970) and in contrast to the value 7.1 that is commonly given.

Kanamori and Jennings (1978) have recently developed a method of determining Richter local magnitude from strong motion records. Their magnitude assignments are in general agreement with ours. The largest difference is for the Puget Sound earthquake of 1949 for which their value is 6.5 in contrast with our value of 7.1.

We assign recording sites to one of two categories, "rock" or "soil", by applying our best judgment to the available site descriptions. We assign stations to the rock category if they are underlain by material described by such terms as "granite," "diorite," "gneiss," "chert," "graywacke," "limestone," "sandstone," "siltstone," or "shale." Stations are assigned to the soil category if they are underlain by sufficient thickness of material described by such terms as "alluvium," "sand," "gravel," "clay," "silt," "mud," "fill," or "glacial outwash." If we judge from the site description that soil material overlying rock is less than 4 to 5 meters thick we assign the site to the rock category. Sources for site descriptions are given in the table of "strong-motion data". Because considerable uncertainty and ambiguity attends the geological classification of recording sites, we do not even suggest conclusions that rely on the validity of the classification of a single station. We are concerned only with trends revealed by comparing whole classes of data.

Many of the data come from the basements or ground floors of buildings or from the abutments of dams. In the analysis of strong-motion data, it is commonly assumed that the influence of the structure on the motion of the base can be ignored and that the data as recorded represent free-field ground motion. We have attempted a limited test of this assumption by classifying recording sites in accordance with the size of the associated structure; class 1 for sites at the base of one- or two-story buildings and class 2 for sites at the base of taller buildings or on dam abutments. Comparison of the two classes using data from the San Fernando earthquake is described in a subsequent section.

With regard to velocity and displacement, one would expect the data from small structures to be more representative of free-field motion. The transfer functions relating motion at the base of structures to

free-field motion tend toward unity for frequencies that are small compared to the fixed-base natural frequencies of the structure. (For examples of theoretical and empirical transfer functions see Duke and others, 1970, and Crouse and Jennings, 1975). The small structures have natural frequencies mostly in the range of 2 to 10 Hertz, which is significantly above the range of frequencies dominant in the velocity and displacement time histories. The case of acceleration is more complicated. For large buildings the dominant frequencies will be higher than the structural resonant frequency, and the transfer functions tend to fall below unity. The natural frequencies of the small structures, however, are in the same range as the frequencies dominant in the acceleration time histories, and the effect of the structure may be to raise or lower the acceleration depending on the spectrum of the earthquake and the details of the transfer function. We would expect the acceleration values for the large structures to be systematically biased downward, but the values for the smaller structures may be either increased or decreased. In fact, our comparison of San Fernando data shows smaller accelerations on the average for the large structures. Our main emphasis, therefore, is placed on the data from the small structures as a basis for estimating free-field motion, but for the horizontal component data we also provide plots and regression parameters for the whole data set.

Geographical distribution. -- In an attempt to keep the data sample reasonably homogeneous, only records obtained in the western part of North America were included. In order to avoid bias from the extremely dense cluster of instruments in downtown Los Angeles a special selection procedure was used in the area between latitude 34.00° and 34.11° N. and longitude 118.24° and 118.45°. Within each of the two geologic site categories, only one recording per earthquake was allowed for each structure category, making a maximum of four possible recordings from the designated area for one earthquake. Selection was made by choosing the station with the smallest identification number of all eligible stations. In the table "strong-motion data", stations so chosen are denoted by an asterisk.

Presentation of data. -- Peak horizontal acceleration, velocity, and displacement data are plotted against distance on log-log grids for each magnitude class. The peak values for horizontal motion are taken from the component with the larger peak. Duration values are plotted against distance on a linear grid. The measure of duration used is the time interval between the first and last horizontal acceleration peaks equal to or greater than 0.05g. The value is taken from the horizontal component that gives the larger value. This is the definition used by Page, Boore, Joyner,

and Coulter (1972). It is a relatively crude measure, but it is simple to determine and is of some value in characterizing ground motion. Peak vertical acceleration, velocity, and displacement are plotted on log-log grids in the same way as the horizontal data.

Statistics. -- The nature of the strong motion data set is not such as to bear the weight of elaborate or subtle statistical inferences. For that reason we emphasize plots showing the individual data points. We do, however, indulge in statistical analysis to the extent of determining least-squares straight lines relating the logarithm of the peak parameters to the logarithm of distance and determining the confidence limits for the prediction of a single value of the dependent variable (Dixon and Massey, 1957). The equations used in the statistical analysis and the coefficients for the regression lines shown in the figures are contained in the "statistical parameters" section (end of the report).

We have attempted to avoid bias in the regression analysis by not including points that are either too close or too far from the fault. In the first case the data are too sparse to indicate the proper functional form for the regression and in the second the data set is incomplete because not all instruments were triggered by the motion. For small structures the data used in our regression calculations are contained within the ranges 5-30, 15-55, and 40-150 km for magnitude classes 5.0-5.7, 6.0-6.4, and 7.1-7.6, respectively. For the San Fernando earthquake the range is 15-100 km. For the whole data set, including both large and small structures, the ranges are the same as for the small structures except for magnitude class 6.0-6.4 for which the range is 10-55 km.

The straight lines obviously fit the data as well as would any simple relation. Curvature that might be caused by anelastic attenuation is completely obscured by the scatter in the data.

The scatter is approximately constant independent of distance. This constancy suggests that the decision was correct to fit a straight line relation to the logarithms of variables rather than fit a power law relation to the variables themselves.

ALL EARTHQUAKES

Data for all the earthquakes are presented in this section, with emphasis on the data from small structures because, for reasons given previously, we consider those data a better guide to free-field motion. In the succeeding section data from the San Fernando earthquake are examined to assess the effect of structure and the effect of local site geology.

Horizontal acceleration. -- Peak horizontal acceleration data from the small structures for the three magnitude classes (figs. 1-3) show that accelerations clearly increase with magnitude in those distance ranges for which there is overlap between the classes. The relations among the magnitude classes are summarized in figure 4, which shows the overlap of the 70 percent prediction intervals. The scatter for the magnitude 5.0-5.7 data is significantly greater than that for either of the other two classes. This difference may arise partly because a number of different earthquakes contribute substantially to the data set for the 5.0-5.7 class, whereas the 6.0-6.4 class is dominated by data from the 1971 San Fernando earthquake and the 7.1-7.6 class is dominated by data from the 1952 Kern County earthquake.

The rate of attenuation of acceleration with distance for the magnitude 5.0-5.7 class appears to be greater than indicated by the slope of -0.9 for the mean regression line in figure 1. This is suggested by the systematic tendency for the data points at distances beyond 30 km to lie below an extension of the mean regression line. As previously explained, we have chosen to exclude from the regression analysis data beyond the distance at which all instruments can be presumed to have triggered. The distance range for which a reasonably complete data set is currently available is not adequate for a good determination of slope; the standard error of the slope for the magnitude 5.0-5.7 class is 0.5. Judging from the data at greater distances, the slope of -1.2 ± 0.3 for the mean line for the magnitude 6.0-6.4 class (fig. 2) appears to be a better estimate of the rate of attenuation to distances of at least 100 km for that data set. The slope of -2.0 ± 0.4 for the magnitude 7.1-7.6 class (fig. 3) may overestimate the rate of attenuation, but the data are scanty.

Horizontal velocity. -- The peak horizontal velocity data from the small structures for the three magnitude classes are presented in figures 5-7. There are fewer velocity than acceleration points because integrations were not available for all the accelerograms. There are so few points for the magnitude 7.1-7.2 class that regression lines are not included on figure 7. As with acceleration, the peak velocity at a given distance tends to increase with magnitude (fig. 8).

The slope of -0.6 ± 0.4 for the mean regression lines for the magnitude 6.4 data appears to underestimate the rate of attenuation if one considers the San Fernando data (described in the next section), which give better determinations because the distance range extends to 100 km. We were

confident that all the instruments out to 100 km were triggered in the San Fernando earthquake, but this confidence does not apply to the whole magnitude class.

Horizontal displacement. -- The peak horizontal displacements for the three magnitude classes are given in figures 9-11. The scatter of the data is larger than for acceleration or velocity in each magnitude class, and the standard errors of the slopes of the mean regression lines exceed 0.5. The displacements are derived from double integration of high-pass filtered accelerograms and therefore represent high-pass filtered versions of the true ground displacement. The longer periods, which are contaminated by processing noise, are removed.

Hanks (1975) has studied the errors in displacement records derived by double integration of filtered accelerograms. He found that the errors are typically less than 1 cm in the period range 5-8 s, 1-2 cm at periods near 10 s, and 2-4 cm in the period range 10-15 s. These findings raise the possibility that some of the low-amplitude data points in figures 9 and 10 may be influenced by noise and may represent upper bounds to the actual ground displacement. The character of some of the low amplitude records resembles noise rather than signal. Nevertheless, we have proceeded in the analysis with the understanding that the results may be compromised to some extent by the effect of noise on the weaker motions.

The overlap of the 70 percent prediction intervals for the three magnitude classes is shown in figure 12. The amplitude increases with magnitude.

Duration. -- All the horizontal duration data are plotted in figure 13. Symbols for zero duration indicate that the peak acceleration on the record is less than 0.05 g . The upper and lower rows of X's represent zero durations for magnitude classes 6.4 and 5.3-5.7, respectively.

Two features of the data are obvious and expected. The durations increase with increasing magnitude and decrease with increasing distance. The influence of magnitude reflects the larger fault size and consequent increased time of rupture as magnitude is increased. The effect of distance results from the general decrease in amplitude with distance, given that we have used a fixed amplitude in the definition of duration. Had we defined duration in terms of some fraction of the peak amplitude, it is likely that the spreading apart of the seismic phases would have led to an increase of duration with distance.

Vertical data. -- The vertical data are presented in the same manner as the horizontal data. Peak vertical accelerations for the three magnitude classes are shown in figures 14-16; peak vertical velocities are shown in figures 17-19; and peak vertical displacements are shown in figures 20-22.

The whole data set. -- For the horizontal components, data from both large and small structures taken together are presented in figures 23 through 31.

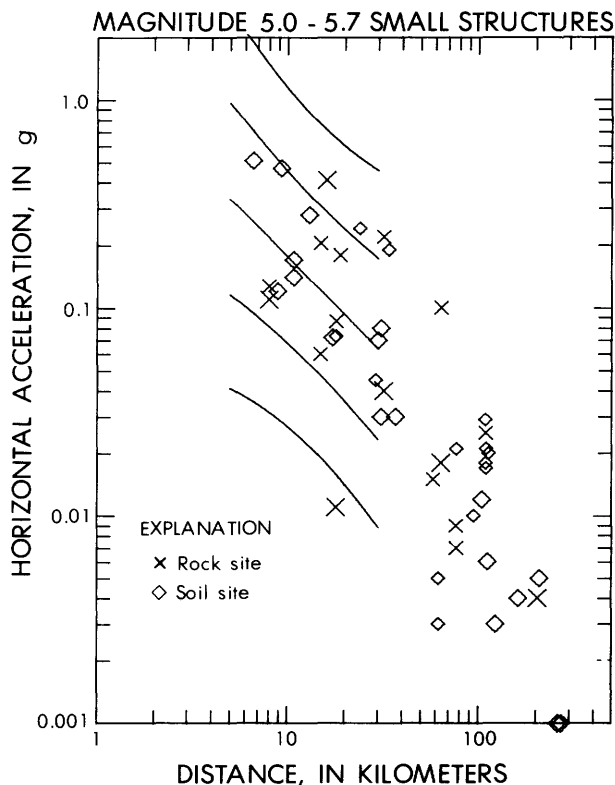


Figure 1. Peak horizontal acceleration versus distance to slipped fault for magnitude range 5.0-5.7 recorded at base of small structures. Center line is mean regression line. Outer pair of lines represents 95 percent prediction interval; inner pair, 70 percent prediction interval. Length of lines represents distance interval considered in regression analysis. Uncertainty in distance is inversely related to symbol size (see text).

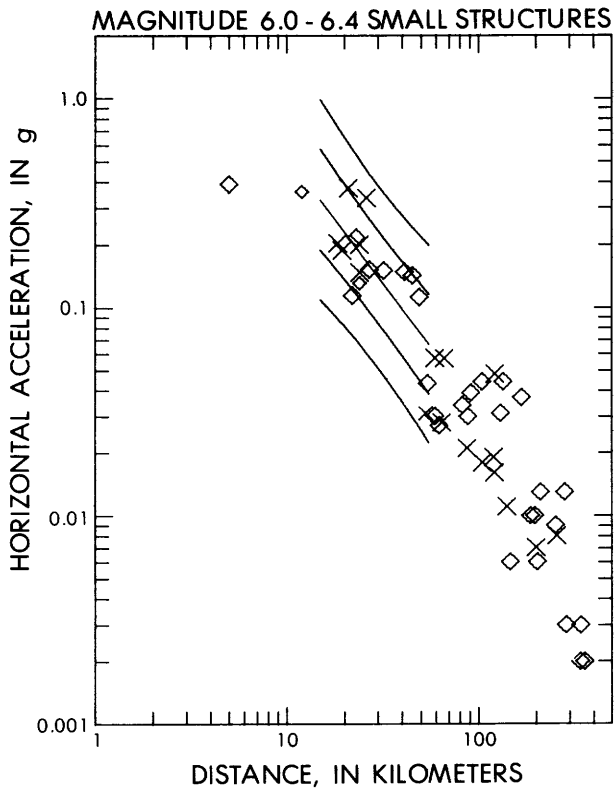


Figure 2. Peak horizontal acceleration versus distance to slipped fault for magnitude range 6.0-6.4 recorded at base of small structures. Symbols and curves same as in figure 1.

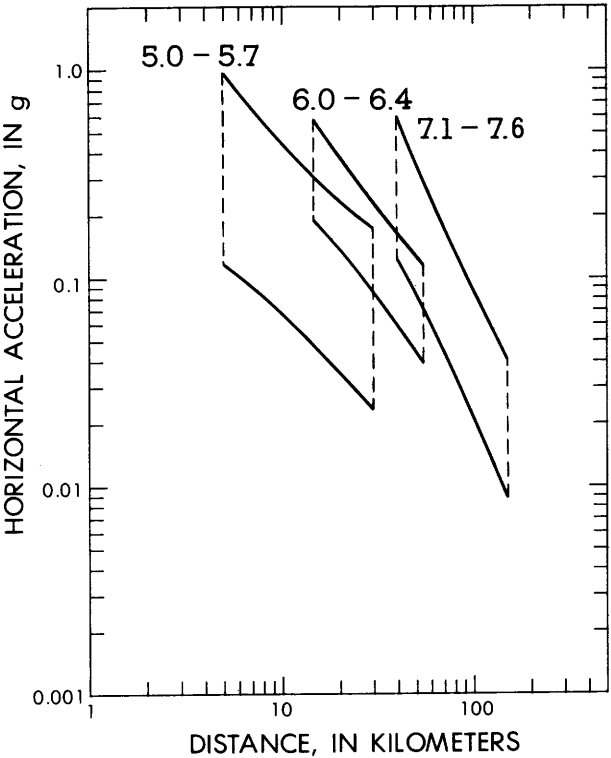
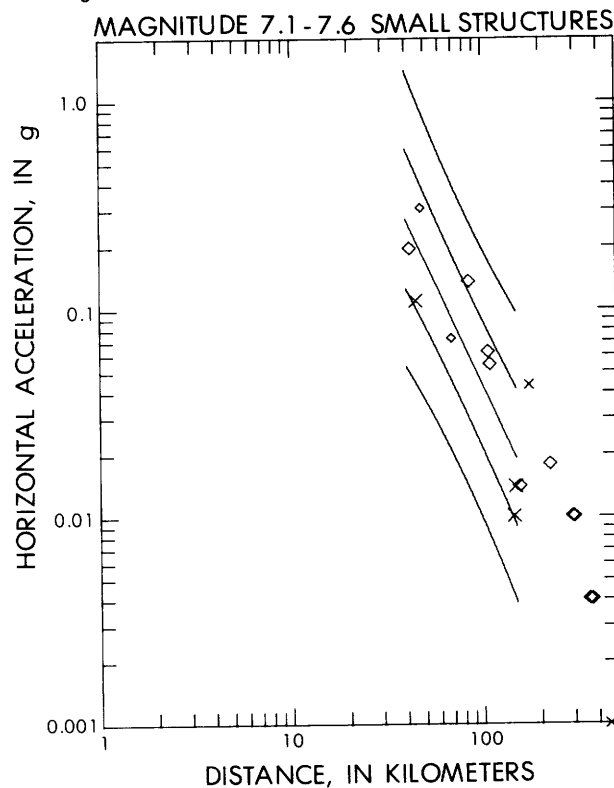


Figure 4. Comparison of 70 percent prediction intervals for peak horizontal acceleration recorded at base of small structures for magnitude classes 5.0-5.7, 6.0-6.4, 7.1-7.6. Curves taken from figures 1-3.

Figure 3. Peak horizontal acceleration versus distance to slipped fault for magnitude range 7.1-7.6 recorded at base of small structures. Symbols and curves same as in figure 1.

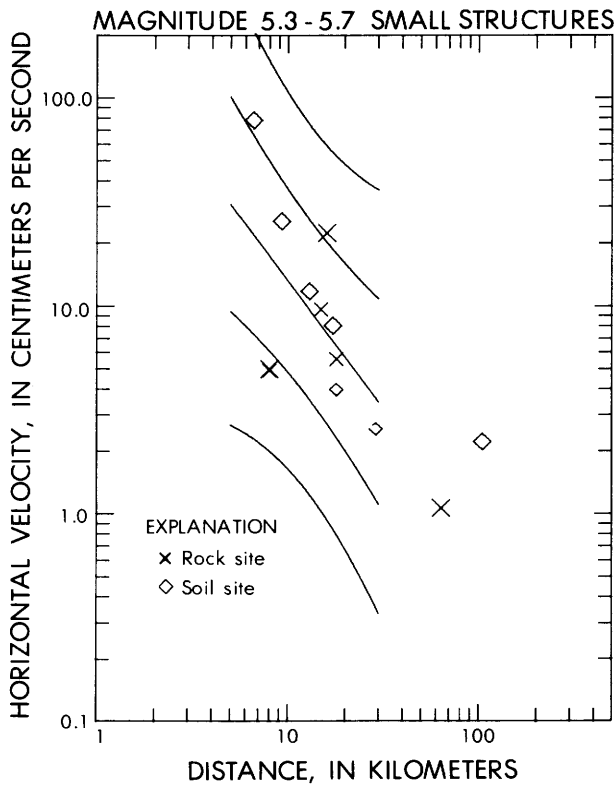


Figure 5. Peak horizontal velocity versus distance from slipped fault for magnitude range 5.3-5.7 recorded at base of small structures. Symbols and curves same as in figure 1.

Figure 7. Peak horizontal velocity versus distance to slipped fault for magnitude range 7.1-7.2 recorded at base of small structures. Symbols same as in figure 1.

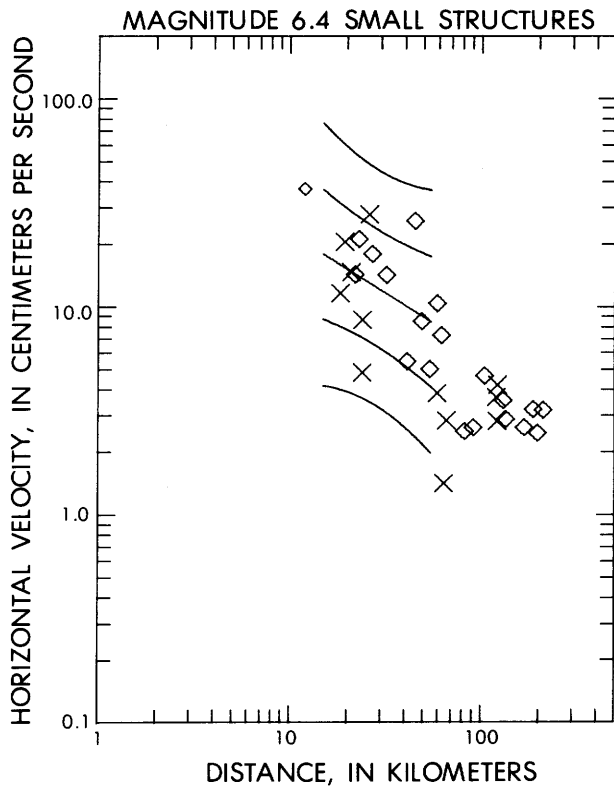
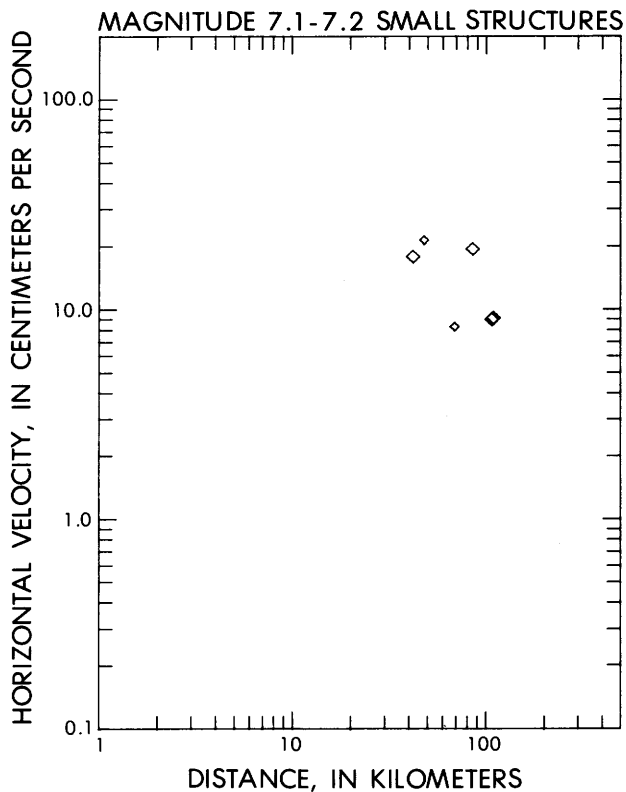


Figure 6. Peak horizontal velocity versus distance to slipped fault for magnitude 6.4 recorded at base of small structures. Symbols and curves same as in figure 1.



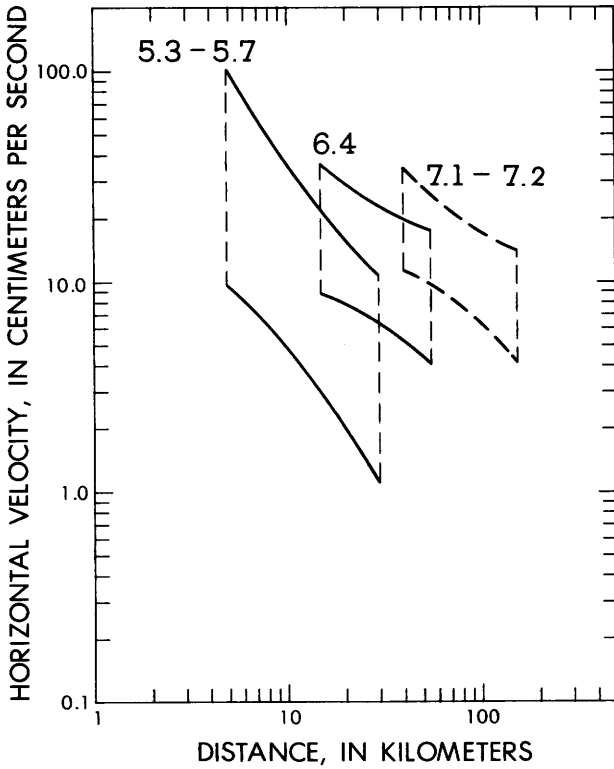


Figure 8. Comparison of 70 percent prediction intervals for peak horizontal velocity recorded at base of small structures for three magnitude classes 5.3-5.7, 6.4, and 7.1-7.2. Curves for magnitude classes 5.3-5.7 and 6.4 taken from figures 5 and 6. Dashed lines for class 7.1-7.2 emphasize uncertainty in slope.

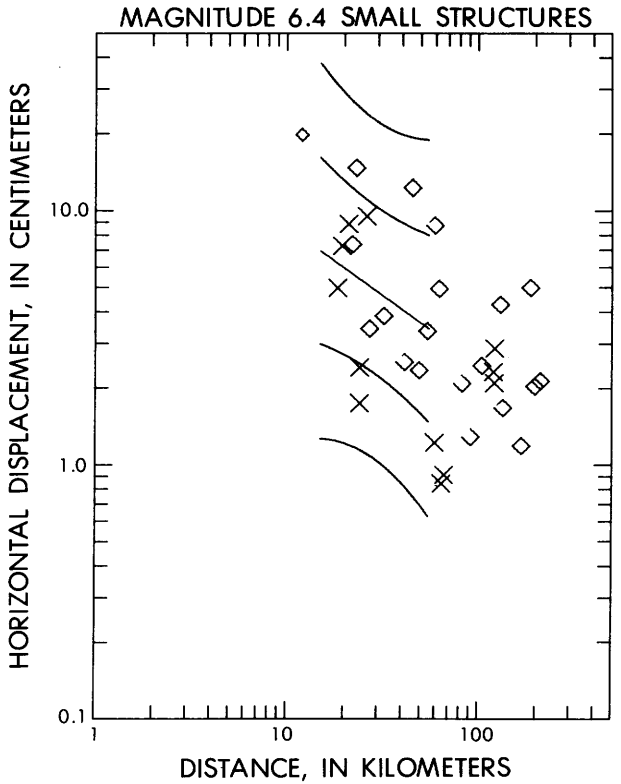
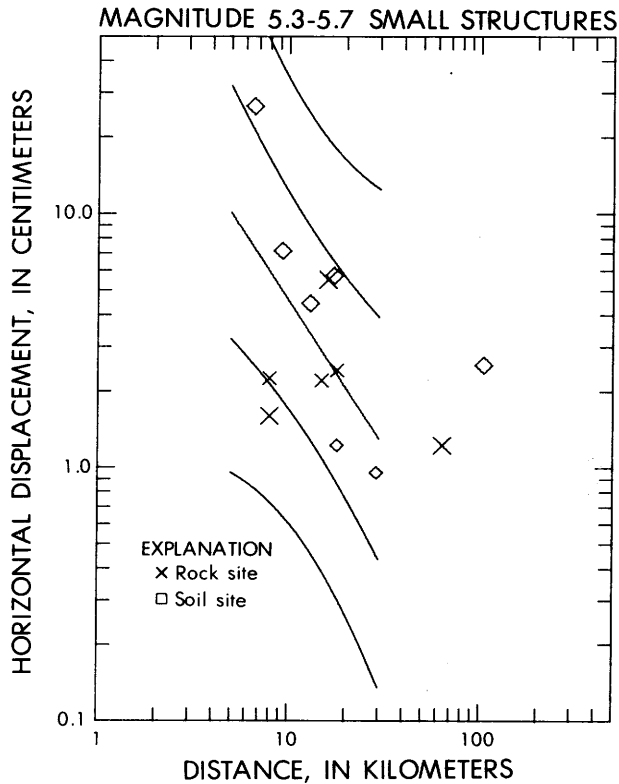


Figure 10. Peak horizontal displacement versus distance to slipped fault for magnitude 6.4 recorded at base of small structures. Symbols and curves same as in figure 1.

Figure 9. Peak horizontal displacement versus distance to slipped fault for magnitude range 5.3-5.7 recorded at base of small structures. Symbols and curves same as in figure 1.

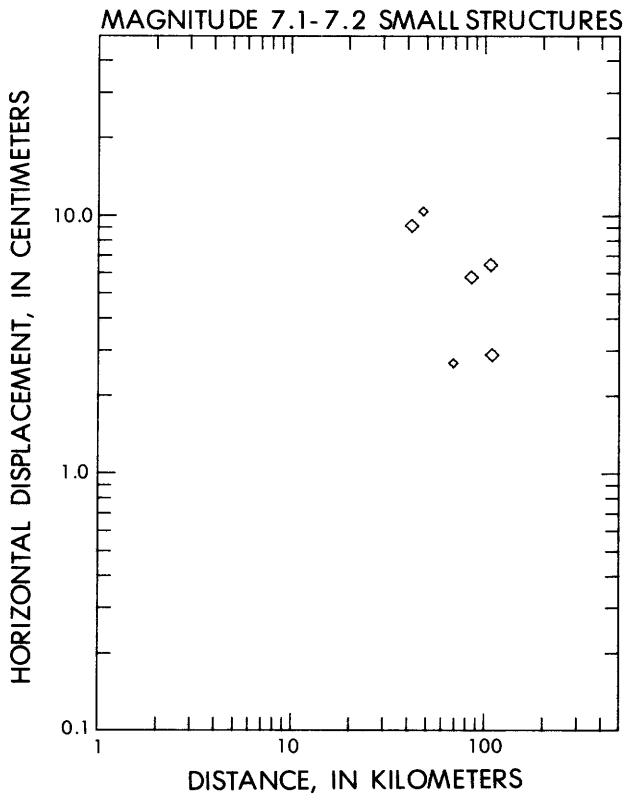


Figure 11. Peak horizontal displacement versus distance to slipped fault for magnitude range 7.1-7.2 recorded at base of small structures. Symbols same as in figure 1.

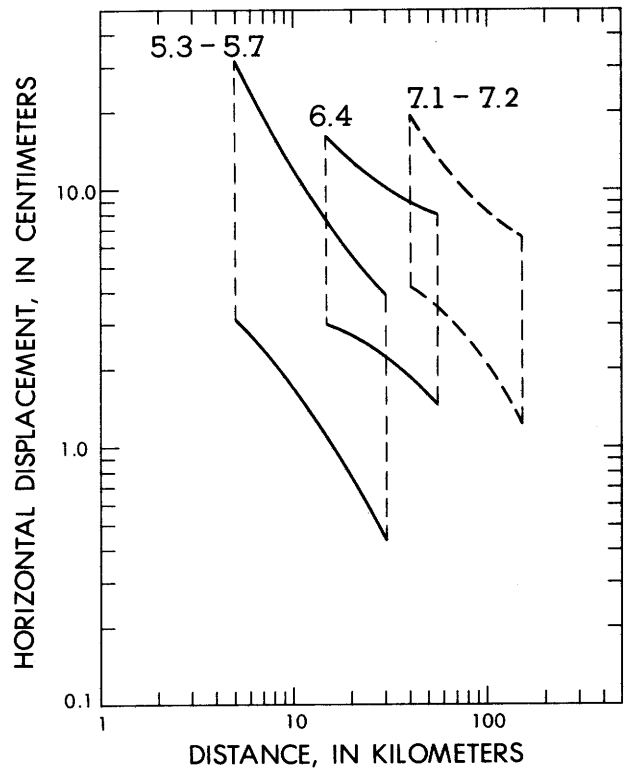


Figure 12. Comparison of 70 percent prediction intervals for peak horizontal displacement recorded at base of small structures for three magnitude classes 5.3-5.7, 6.4, and 7.1-7.2. Curves for magnitude classes 5.3-5.7 and 6.4 taken from figures 9 and 10. Dashed lines for class 7.1-7.2 emphasize uncertainty in slope.

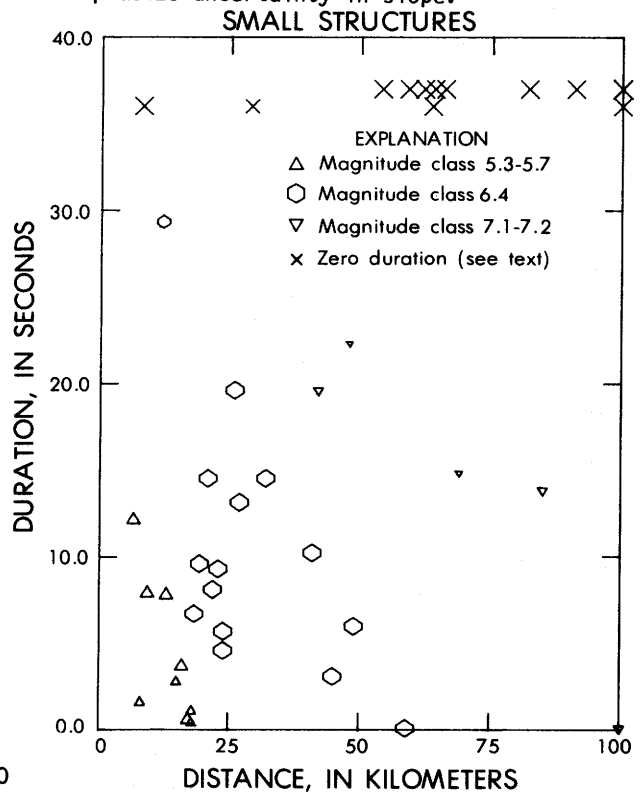


Figure 13. Duration versus distance from slipped fault for recordings from small structures.

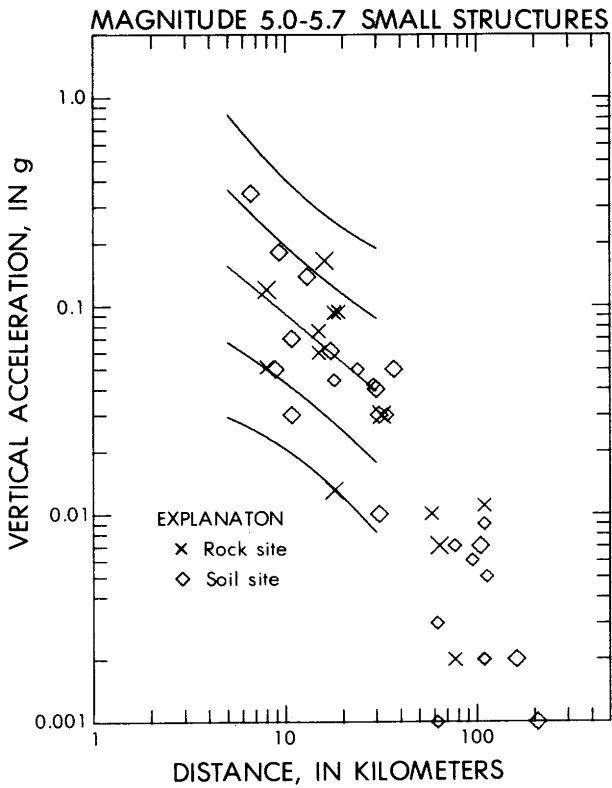


Figure 14. Peak vertical acceleration versus distance to slipped fault for magnitude range 5.0-5.7 recorded at base of small structures. Symbols and curves same as in figure 1.

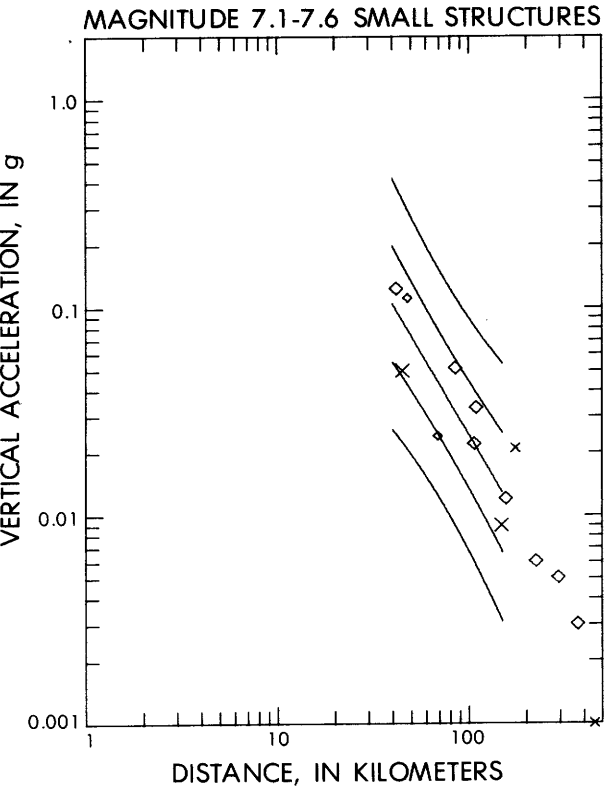
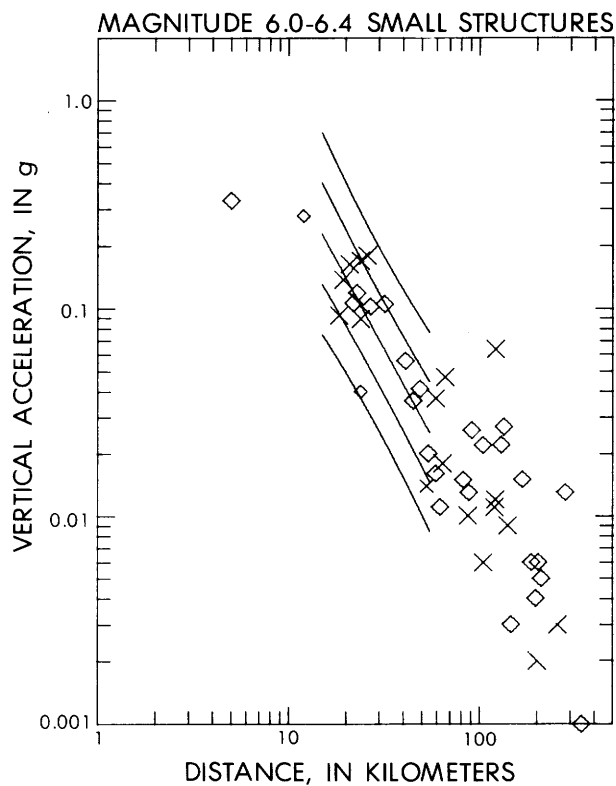


Figure 16. Peak vertical acceleration versus distance to slipped fault for magnitude range 7.1-7.6 recorded at base of small structures. Symbols and curves same as in figure 1.

Figure 15. Peak vertical acceleration versus distance to slipped fault for magnitude range 6.0-6.4 recorded at base of small structures. Symbols and curves same as in figure 1.

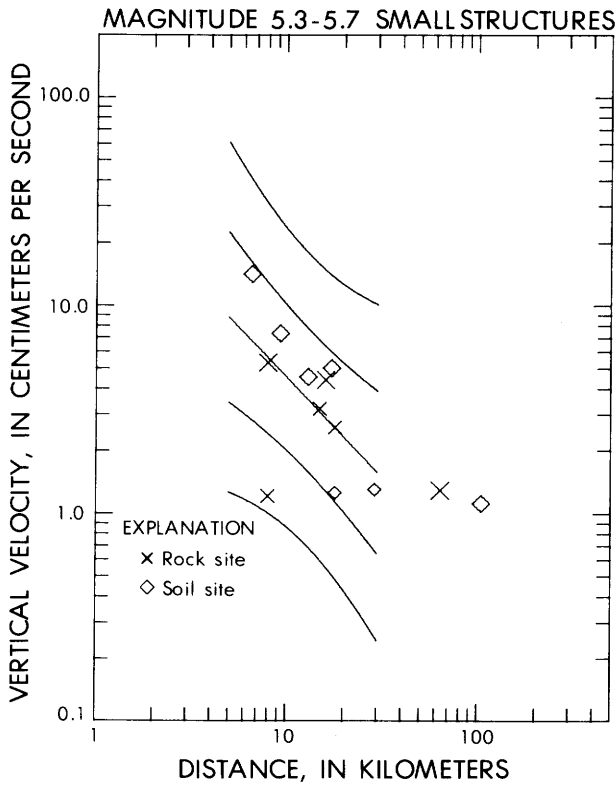


Figure 17. Peak vertical velocity versus distance to slipped fault for magnitude range 5.3-5.7 recorded at base of small structures. Symbols and curves same as in figure 1.

Figure 19. Peak vertical velocity versus distance to slipped fault for magnitude range 7.1-7.2 recorded at base of small structures. Symbols same as in figure 1.

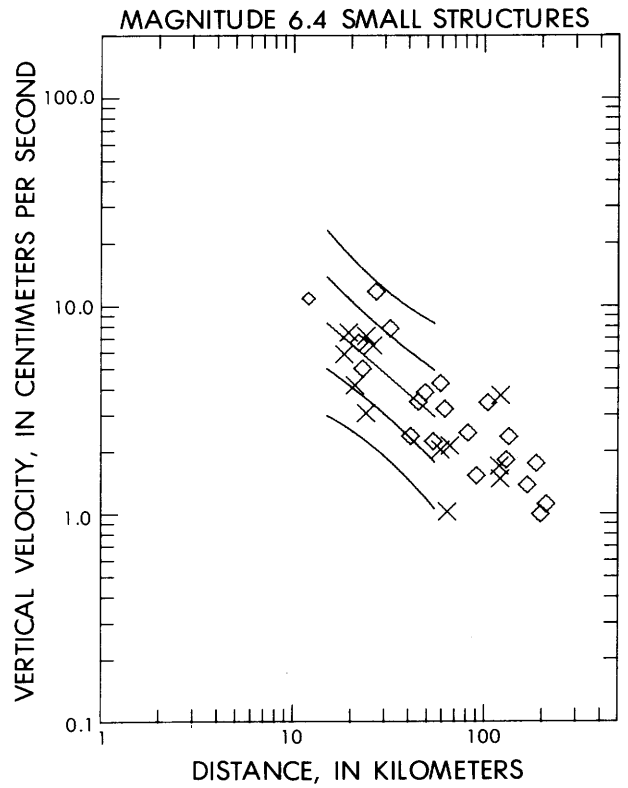
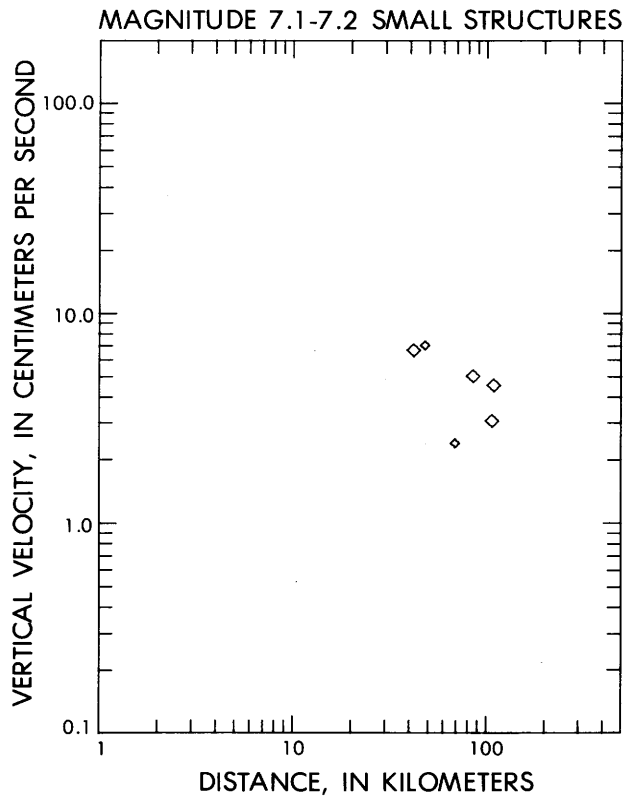


Figure 18. Peak vertical velocity versus distance to slipped fault for magnitude 6.4 recorded at base of small structures. Symbols and curves same as in figure 1.



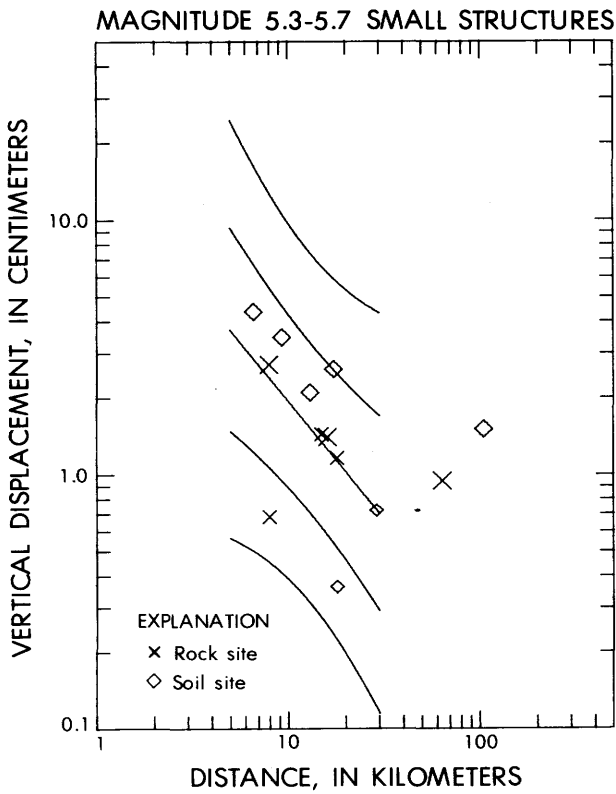


Figure 20. Peak vertical displacement versus distance to slipped fault for magnitude range 5.3-5.7 recorded at base of small structures. Symbols and curves same as in figure 1.

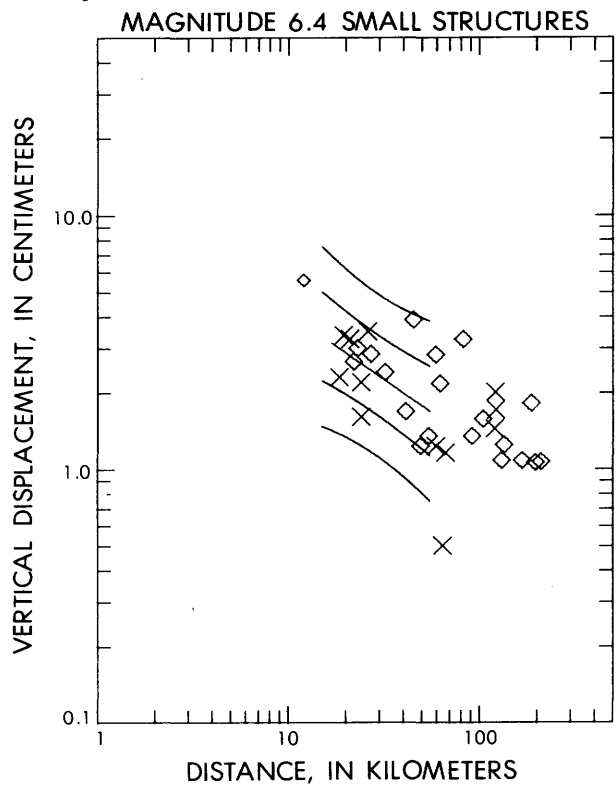


Figure 21. Peak vertical displacement versus distance to slipped fault for magnitude 6.4 recorded at base of small structures. Symbols and curves same as in figure 1.

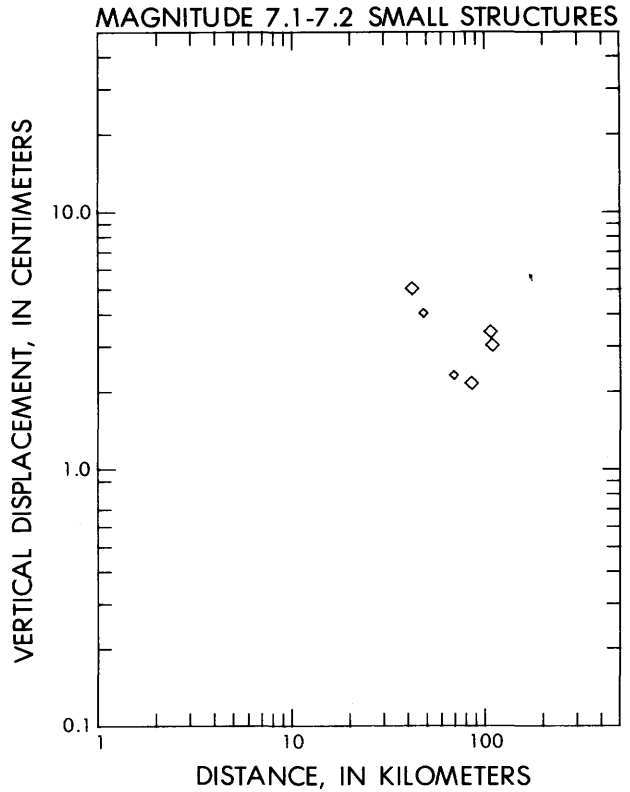


Figure 22. Peak vertical displacement versus distance to slipped fault for magnitude range 7.1-7.2 recorded at base of small structures. Symbols same as in figure 1.

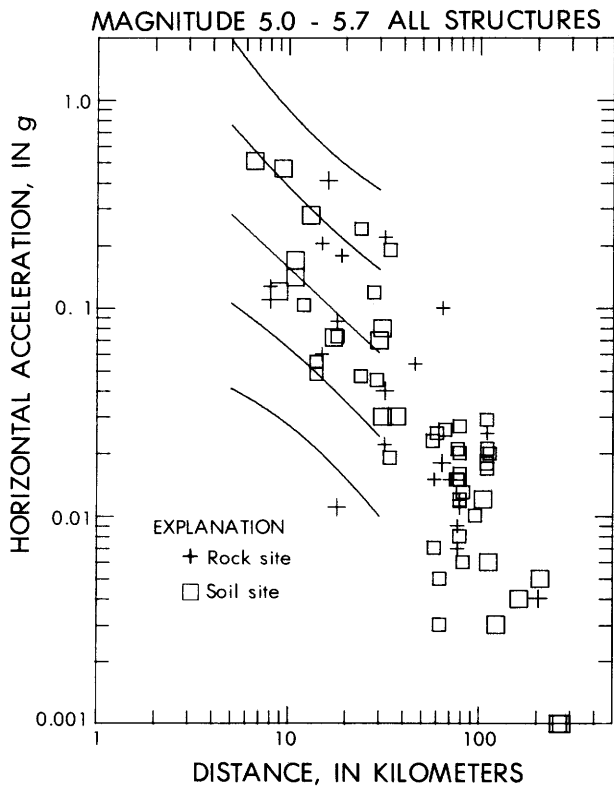


Figure 23. Peak horizontal acceleration versus distance to slipped fault for magnitude range 5.0-5.7 including data from both large and small structures. The center line is the mean regression line. The outer pair of lines represents the 95 percent prediction interval, and the inner pair represents the 70 percent prediction interval. Length of lines represents the distance interval considered in the regression analysis.

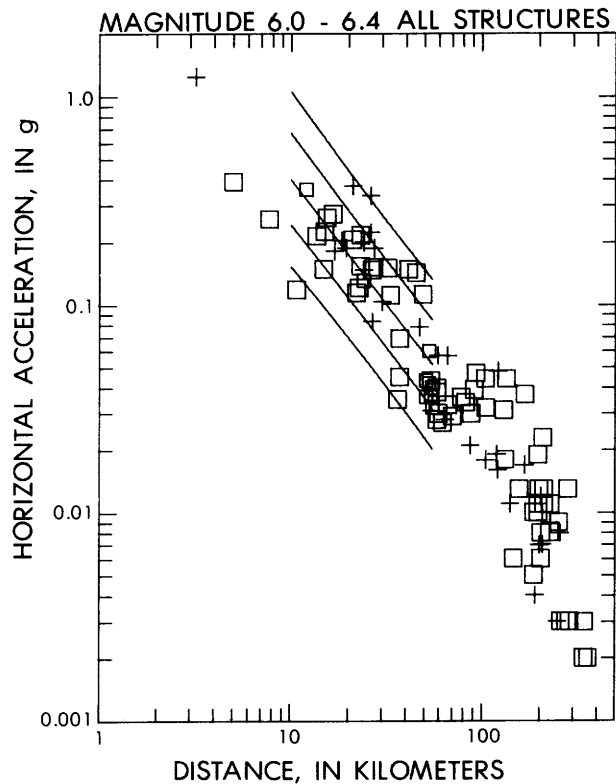


Figure 24. Peak horizontal acceleration versus distance to slipped fault for magnitude range 6.0-6.4 including data from both large and small structures. Symbols and curves same as in Figure 23.

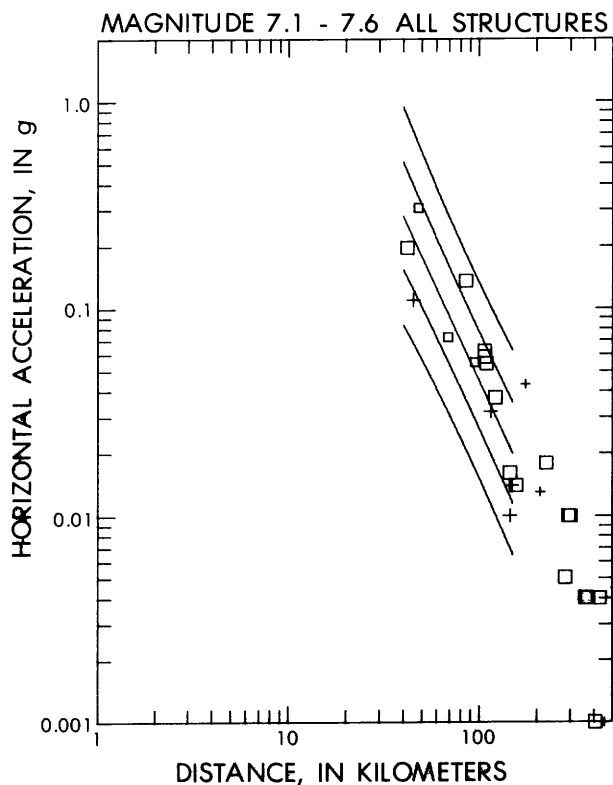


Figure 25. Peak horizontal acceleration versus distance to slipped fault for magnitude range 7.1-7.6 including data from both large and small structures. Symbols and curves same as in Figure 23.

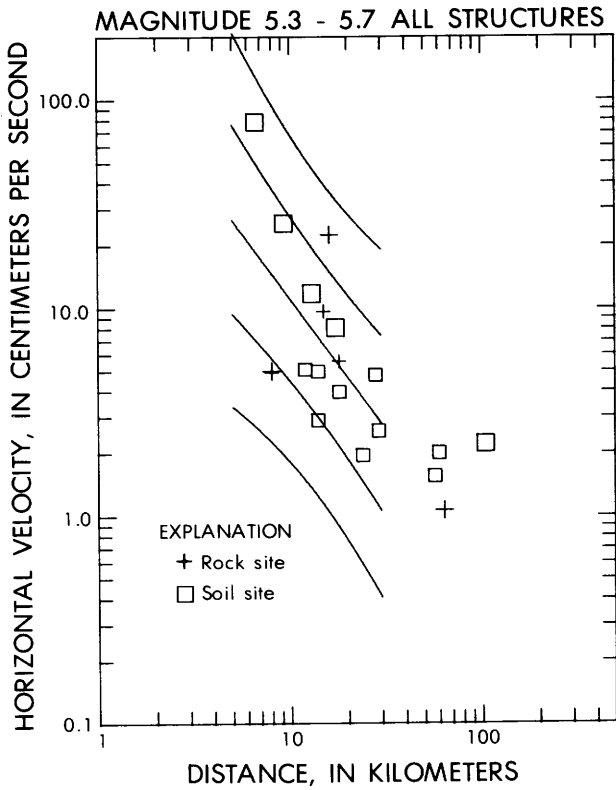


Figure 26. Peak horizontal velocity versus distance to slipped fault for magnitude range 5.3-5.7 including data from both large and small structures. Symbols and curves same as in figure 23.

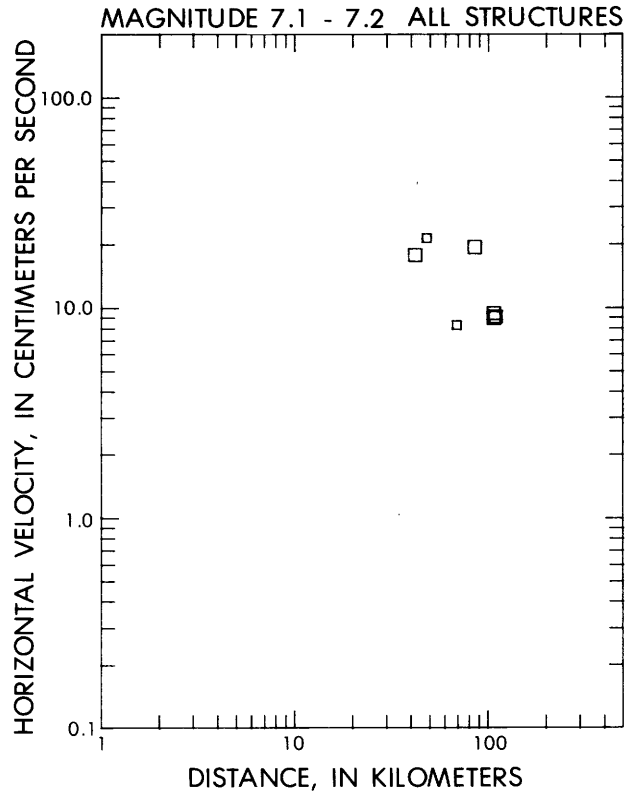


Figure 28. Peak horizontal velocity versus distance to slipped fault for magnitude range 7.1-7.2 including data from both large and small structures. Symbols same as in figure 23.

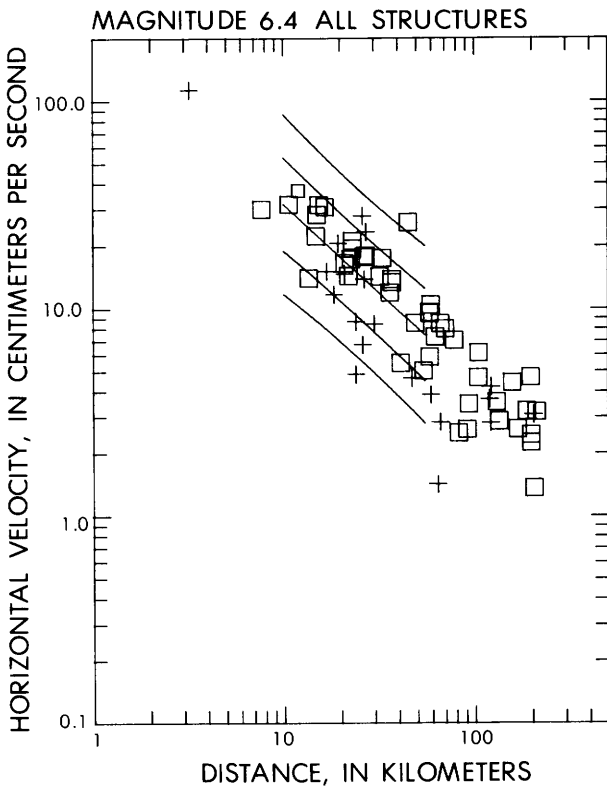


Figure 27. Peak horizontal velocity versus distance to slipped fault for magnitude 6.4 including data from both large and small structures. Symbols and curves same as in figure 23.

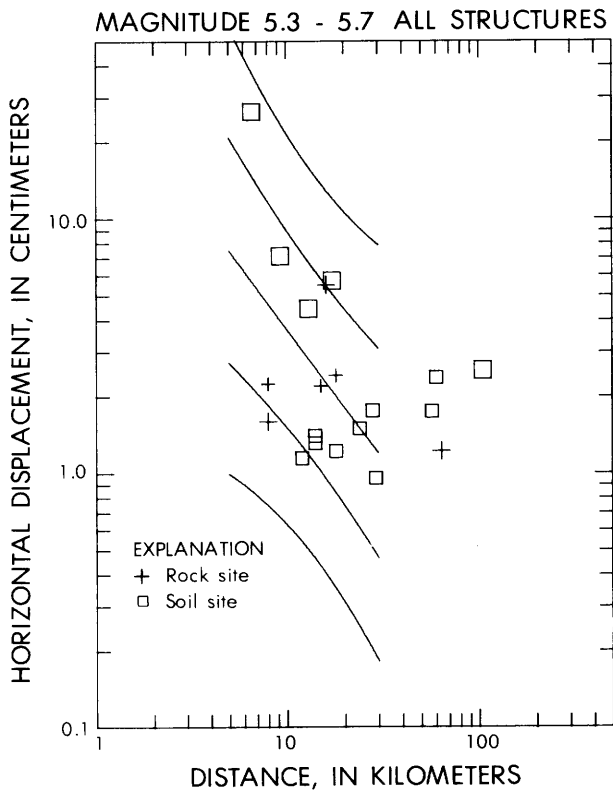


Figure 29. Peak horizontal displacement versus distance to slipped fault for magnitude range 5.3-5.7 including data from both large and small structures. Symbols and curves same as in figure 23.

Figure 31. Peak horizontal displacement versus distance to slipped fault for magnitude range 7.1-7.2 including data from both large and small structures. Symbols same as in Figure 23.

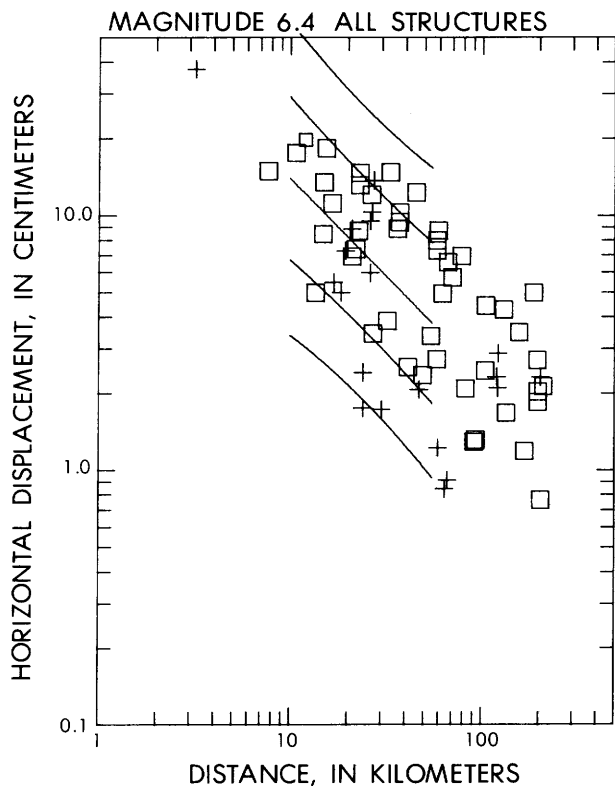
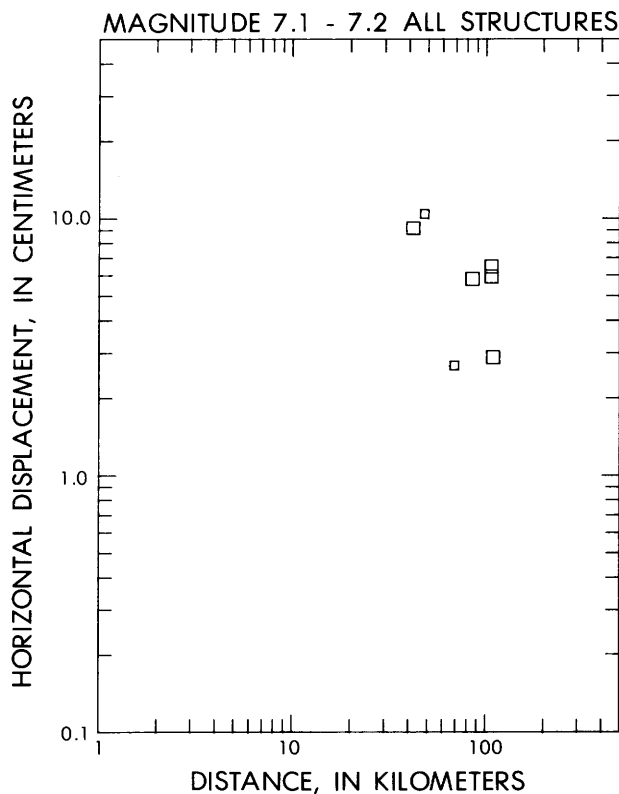


Figure 30. Peak horizontal displacement versus distance to slipped fault for magnitude 6.4 including data from both large and small structures. Symbols and curves same as in figure 23.



SAN FERNANDO EARTHQUAKE

The San Fernando earthquake supplied more than one-quarter of the total data points in our sample. The large number of data points from a single event provides the best basis for examining the effect of structure and local site conditions. The San Fernando earthquake also gives more accurate values than the whole magnitude 6.0-6.4 data set for the slopes of the regression lines for peak parameters against distance. This accuracy is possible because, as mentioned previously, the statistical analysis can be carried out over a greater range of distance for the San Fernando earthquake. As discussed earlier, to avoid bias not all the records from downtown Los Angeles are included in the data set.

In comparing peak parameters for different structural types and site conditions, we use an analysis of variance technique (Acton, 1959, p. 80-83) to test the statistical significance of the observed differences between one data set and another. To state the matter more precisely, we consider the variance of the residuals and examine the statistical significance of the reduction in variance that occurs when different regression lines are fit to the two different data sets. The technique allows us to break down the reduction of variance into a component attributable to separate slopes and a component attributable to separate means. In what follows, when we say a difference is significant we mean that it corresponds to a significant reduction in the variance of the residuals. In general, the analysis of variance tests enable us to see how the differences between data sets compare with those that might be caused by random sampling error. We should not be confident, however, that the strong-motion data sets represent random samples, and, in any case, the statistical tests say nothing about the real physical meaning of the differences between data sets.

Effect of structure. -- Figure 32 compares peak horizontal acceleration values recorded on soil at the base of small structures (S1) and large structures (S2). Figure 33 shows the mean regression lines and the 70 percent prediction intervals determined separately for the S1 and S2 data. The mean regression line for the S1 data lies above that for the S2 data, and the analysis of variance tests indicate that the difference is significant at the 90 percent level. The difference in slope is not significant. The same comparisons are made for horizontal velocity in figures 34 and 35. For velocity, the mean regression line for the S1 data lies generally below that for the S2 data, although they cross, and the difference is statistically significant at the 98 percent level, though unimpressive to the eye. The S1 line is steeper, and the

difference in slope is significant at the 90 percent level. The horizontal displacement data (fig. 36 and 37) show that the mean regression line for the S1 data lies below that for the S2 data, and the difference is significant at the 99 percent level. The difference in slope is not significant.

In summary, for most of the distance range covered by the regression analysis peak horizontal acceleration is less and peak horizontal velocity and displacement are greater, on the average, at the base of large structures than at the base of small structures. The attenuation with distance is greater for the small structures for all three parameters, but the difference is statistically significant only for peak velocity. The result that acceleration values from the large structures are lower on the average is what would be expected if soil-structure interaction biases those data downward. This result encourages us in our preference for the data from small structures as a basis for estimating free-field ground motion. In general, however, the differences between the data from the large structures and the small structures are relatively small compared with the range of either data set, and we do not believe that firm conclusions are warranted solely on the basis of formal statistical tests. The differences may be due to soil-structure interaction, but more study would be required to demonstrate this.

Effect of site geology. -- Figure 38 compares peak horizontal acceleration recorded at the base of small structures on rock and soil. Figure 39 shows the mean regression line and 70 percent confidence intervals determined separately for the two data sets. The analysis-of-variance tests indicate that the differences are not significant in either slope or level. Peak horizontal velocity data for small structures on both rock and soil sites (figs. 40 and 41) show that the mean regression line is higher for soil, and that difference is significant at the 98 percent level. The difference in slope is not significant. Peak horizontal displacement data (figs. 42 and 43) show that the mean regression line for soil is higher, and that difference is significant at the 98% level. The difference in slope is not significant even at the 75 percent level.

Apparently, peak horizontal acceleration is nearly the same, on the average, on rock and soil sites, whereas both peak horizontal velocity and displacement are larger on soil sites. This relation is not the result of any obvious bias in the data. No gross effect is evident from bias in the distribution of stations with distance. To test for bias due to the nonuniform azimuthal distribution of the data (Hanks, 1975), we determined the azimuth of each station with respect to a point in the center of the zone of fault

rupture (lat 34.37° N., long 118.42° W.). A mean regression line against distance was determined for all the peak horizontal acceleration data for small structures in the distance range 15-100 km (with distance measured to the closest point on the rupture surface, as before). Residuals to that regression line are plotted against azimuth in a polar diagram (fig. 44). The circle represents zero residual. No strong systematic difference is apparent between rock and soil. Figure 45 gives the corresponding plot for the velocity data. Although the azimuthal coverage is far from complete, we can say that in any range of azimuth for which both rock and soil points are present, the soil residuals are more positive. Similar results are obtained for the displacement data (fig. 46).

We tentatively conclude that amplification of velocity and displacement is a real effect associated with soil sites. We presume that for the soil sites some sort of amplification mechanisms are operating on the longer periods that are dominant on velocity and displacement records. For the shorter periods that are dominant on acceleration records, these mechanisms are counterbalanced by anelastic attenuation. We will not speculate here on the nature of the amplification mechanisms. Similar conclusions on the effect of site conditions on strong motion in the San Fernando earthquake were reported by Duke, Johnsen, Larson, and Engman (1972), Trifunac (1976), and Arnold, Vanmarcke, and Gazetas (1976).

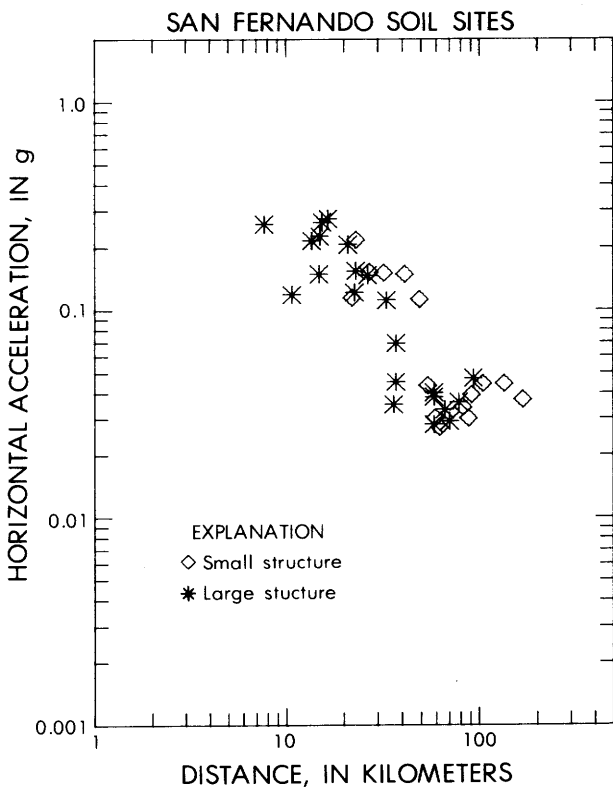


Figure 32. Peak horizontal acceleration versus distance to slipped fault at soil sites in San Fernando earthquake.

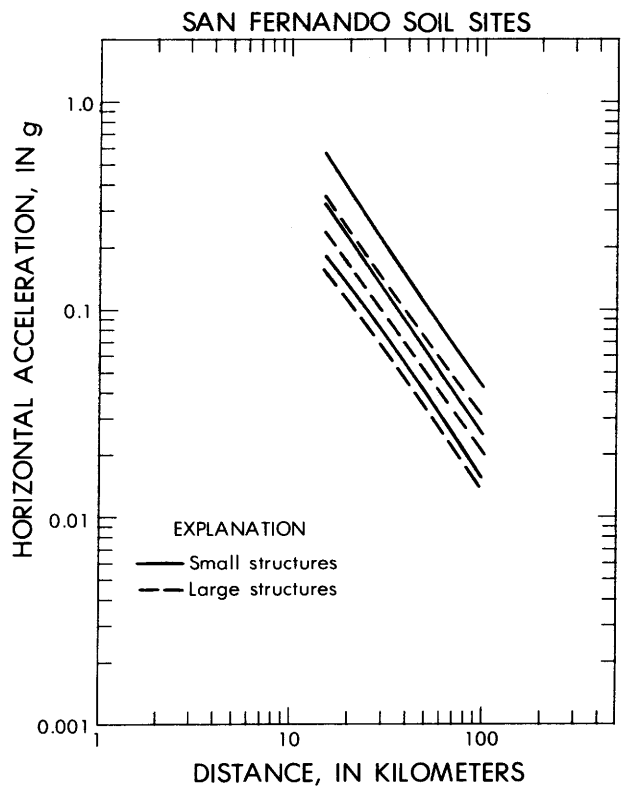


Figure 33. Comparison of mean regression lines and 70 percent prediction intervals for small structures (solid lines) and large structures (dashed lines) for peak horizontal acceleration at soil sites in San Fernando earthquake.

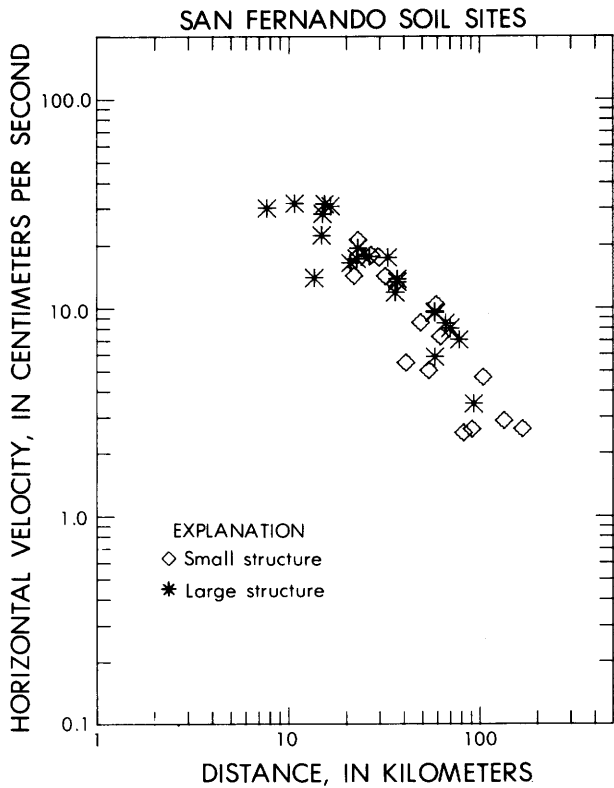


Figure 34. Peak horizontal velocity versus distance to slipped fault at soil sites in San Fernando earthquake. Symbols same as in figure 32.

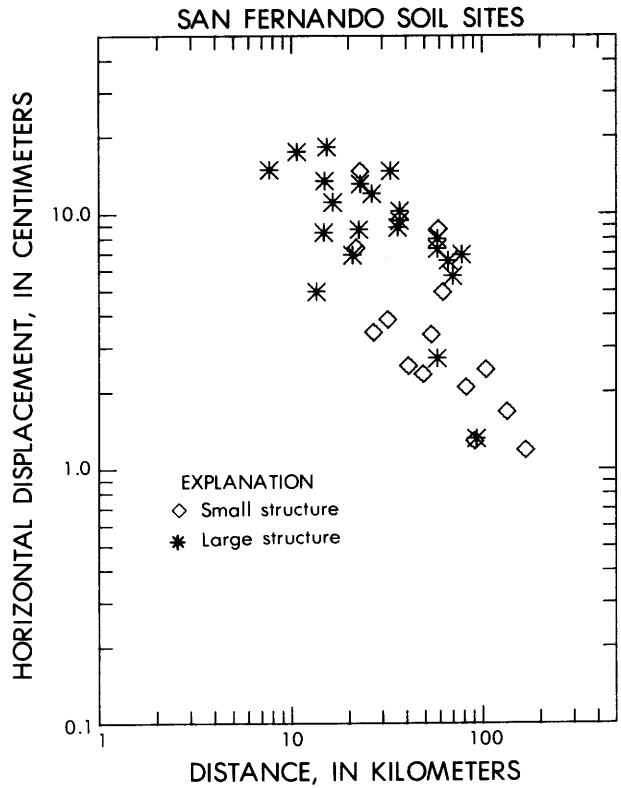


Figure 36. Peak horizontal displacement versus distance to slipped fault at soil sites in San Fernando earthquake. Symbols same as in figure 32.

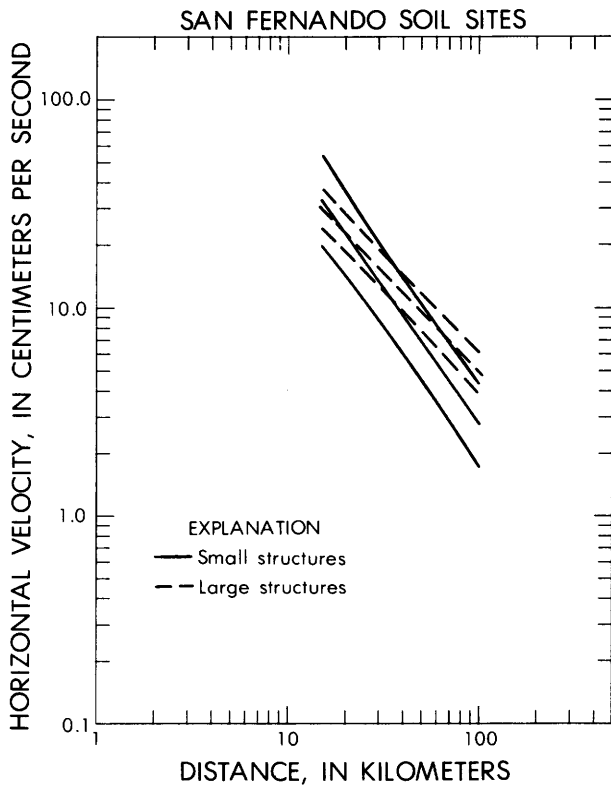


Figure 35. Comparison of mean regression lines and 70 percent prediction intervals for small structures (solid lines) and large structures (dashed lines) for peak horizontal velocity at soil sites in San Fernando earthquake.

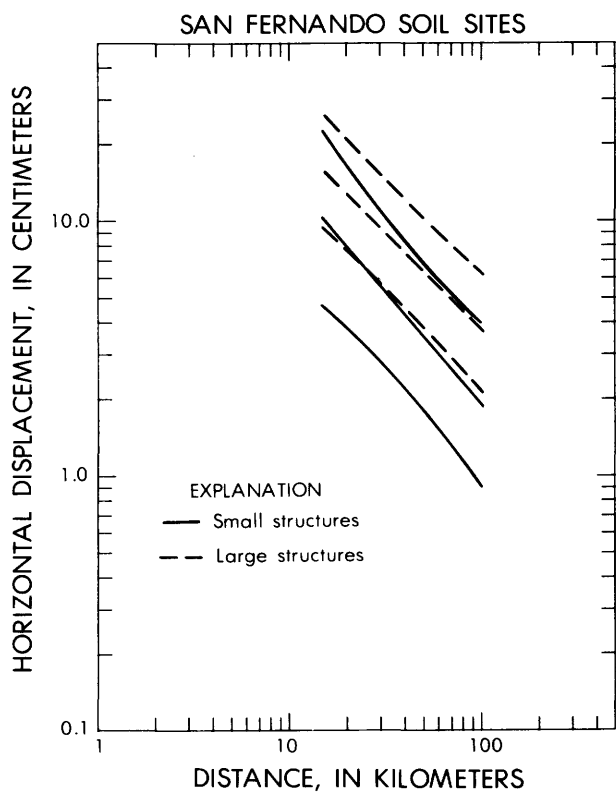


Figure 37. Comparison of mean regression lines and 70 percent prediction intervals for small structures (solid lines) and large structures (dashed lines) for peak horizontal displacement at soil sites in San Fernando earthquake.

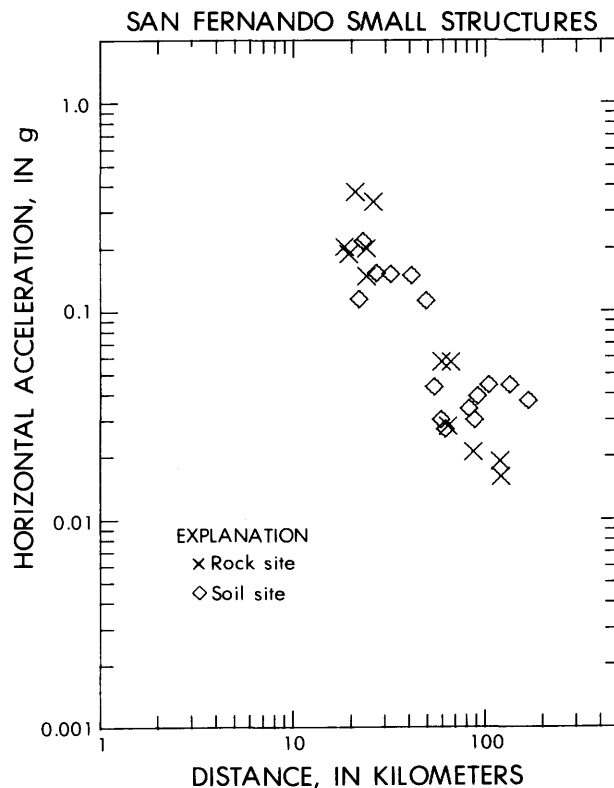


Figure 38. Peak horizontal acceleration recorded at base of small structures versus distance to slipped fault in San Fernando earthquake. Symbols same as in figure 1.

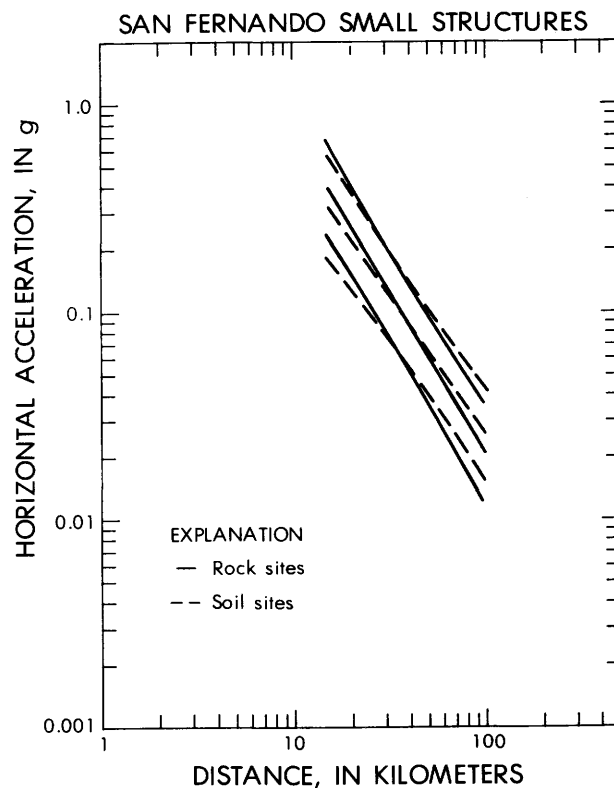


Figure 39. Comparison of mean regression lines and 70 percent prediction intervals for rock sites (solid lines) and soil sites (dashed lines) for peak horizontal acceleration recorded at base of small structures in San Fernando earthquake.

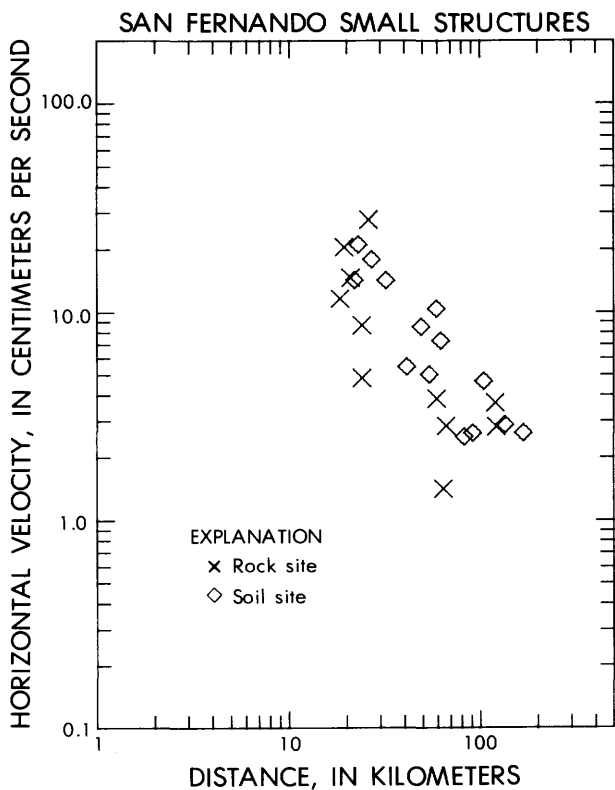


Figure 40. Peak horizontal velocity recorded at base of small structures versus distance to slipped fault in San Fernando earthquake. Symbols same as in figure 1.

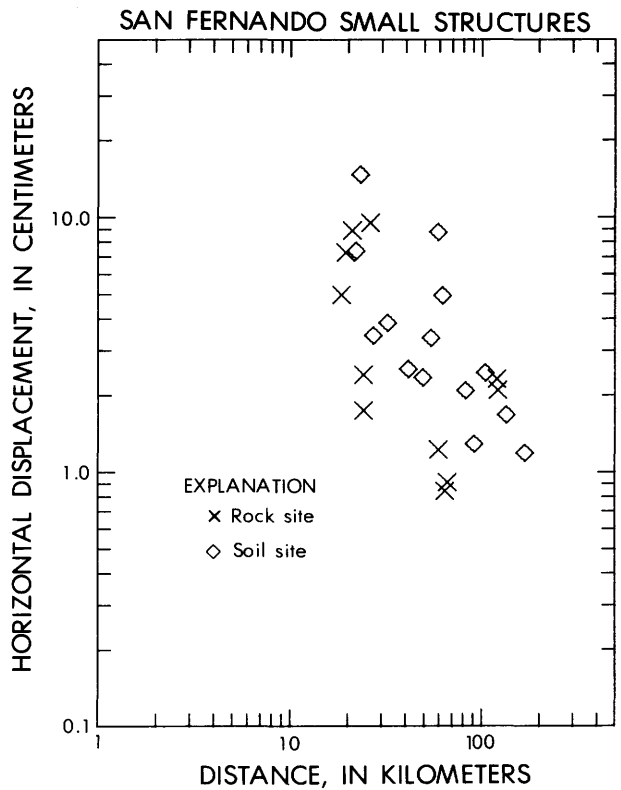


Figure 42. Peak horizontal displacement recorded at base of small structures versus distance to slipped fault in San Fernando earthquake. Symbols same as in figure 1.

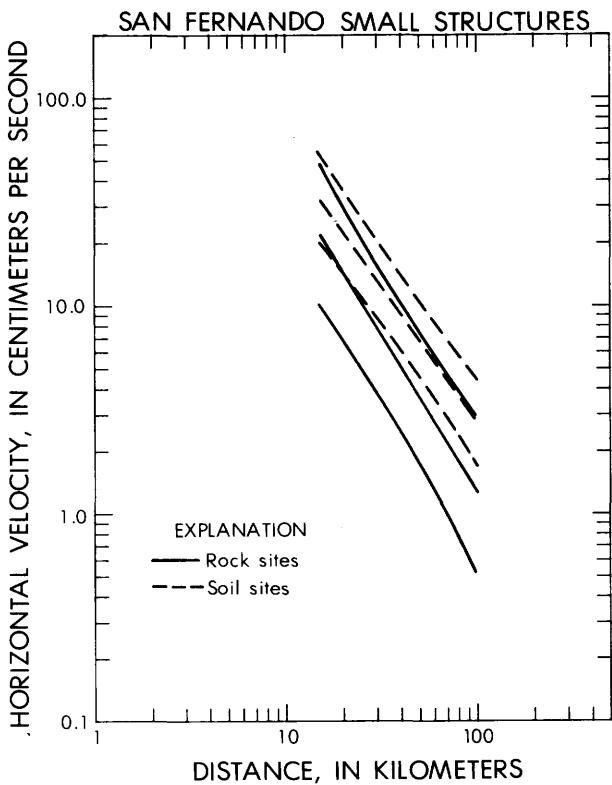


Figure 41. Comparison of mean regression lines and 70 percent prediction intervals for rock sites (solid lines) and soil sites (dashed lines) for peak horizontal velocity recorded at base of small structures in San Fernando earthquake.

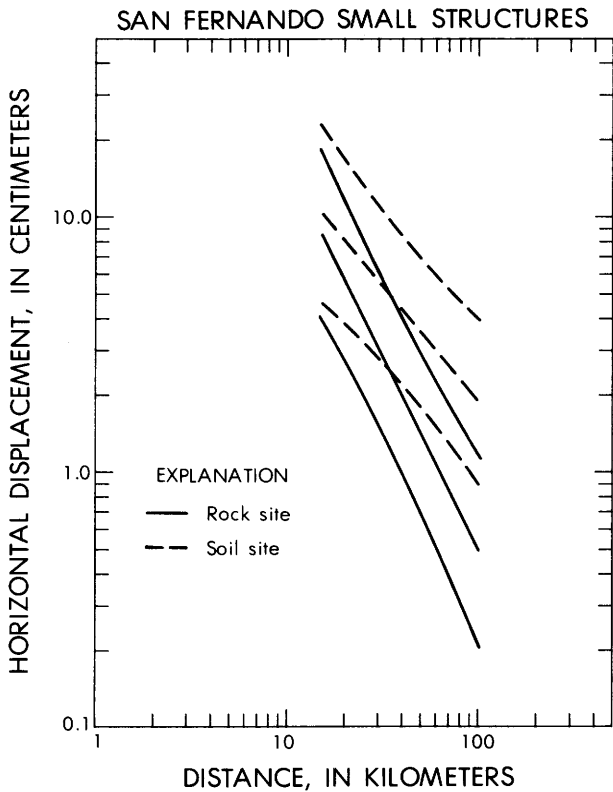


Figure 43. Comparison of mean regression lines and 70 percent prediction intervals for rock sites (solid lines) and soil sites (dashed lines) for peak horizontal displacement recorded at base of small structures in San Fernando earthquake.

Figure 45. Peak horizontal velocity recorded at base of small structures, San Fernando earthquake. Azimuthal dependence of residuals from mean regression line. Symbols same as in figure 44.

SAN FERNANDO
SMALL STRUCTURES ACCELERATION

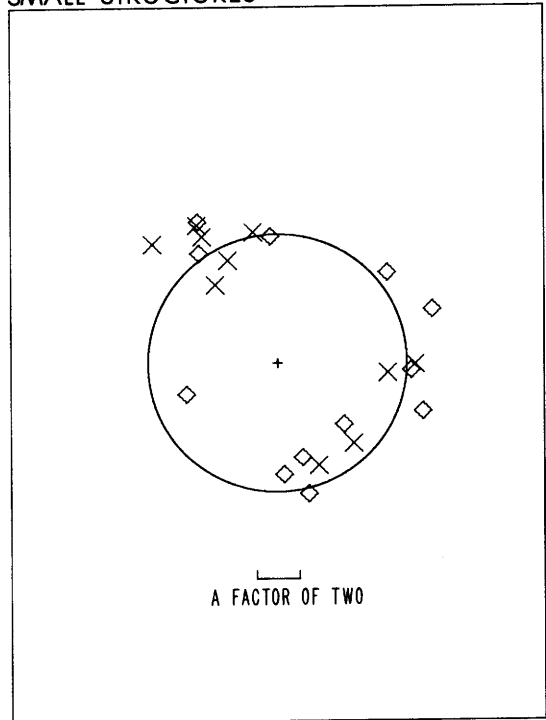
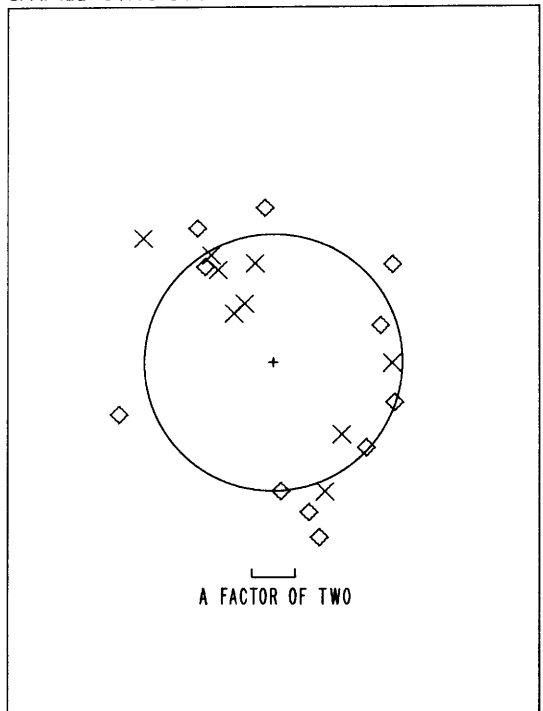


Figure 44. Peak horizontal acceleration recorded at base of small structures, San Fernando earthquake. Azimuthal dependence of residuals from mean regression line. X's and diamonds are rock and soil sites, respectively.

SAN FERNANDO
SMALL STRUCTURES VELOCITY



SAN FERNANDO
SMALL STRUCTURES DISPLACEMENT

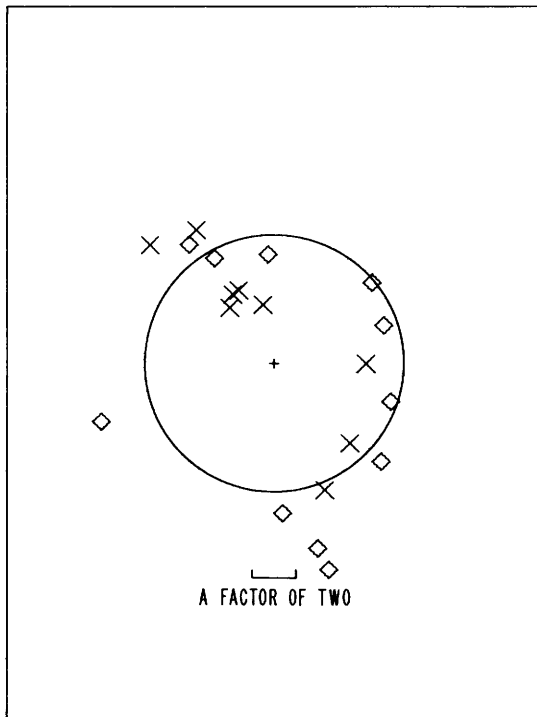


Figure 46. Peak horizontal displacement recorded at base of small structures, San Fernando earthquake. Azimuthal dependence of residuals from mean regression line. Symbols same as in figure 44.

PREVIOUSLY PUBLISHED CURVES
FOR PEAK ACCELERATION

There are a number of published correlations between ground motion parameters and distance, magnitude and site conditions. They have been described by Trifunac and Brady (1976) and discussed by Seed and others (1976). We consider here only three recently published, widely known relations proposed for peak acceleration.

All studies of strong motion data are handicapped by the limited number of data points at small distances from the source. Attempts to predict strong motion parameters at short distance are forced to rely upon rather tenuous assumptions.

Curves for mean peak acceleration are shown in figure 47 for a magnitude 6.6 earthquake. Also shown is the 70 percent prediction interval for the data set for magnitude class 6.0-6.4 and small structures, from this report. Most of the points in that

data set came from the magnitude 6.4 San Fernando earthquake, so the comparison is appropriate from the standpoint of magnitude. Data from large structures, however, were not excluded in the development of the other curves.

The curve labeled "S" was developed by Schnabel and Seed (1973) for rock sites and is based on strong motion data extended to distances nearer the fault with the help of theoretical attenuation curves. Because the theoretical curves are based on the conservation of radiated energy, however, they apply strictly only to quantities related to the energy represented by the whole duration of the seismic record. Application of the curves to peak parameters is an approximation of uncertain accuracy. The measure of distance used by Schnabel and Seed is the shortest distance to the rupture surface, the same measure used in this report.

The curves labeled "T0" and "T2" are the mean curves given by Trifunac (1976) for soft and hard sites, respectively. These curves are based on a data set very similar to the one used in this report, including data from both large and small structures. The distance measure used by Trifunac is epicentral distance. The curves were fitted to the data on the assumption that the distance dependence is that of the function given by Richter (1958) for calculating local magnitudes in southern California. The accuracy of that assumption is difficult to evaluate. Furthermore, the distance function given by Richter is not very well defined for distances between 0 and 20 km, which is the range most important for strong-motion predictions.

The curve labeled "D" was developed by Donovan (1973) for soil sites. It was obtained by fitting 678 data points by a function of the form

$$y = b_1 e^{b_2 m} (R + 25)^{-b_3}$$

where y is peak acceleration, m is magnitude, R is hypocentral distance in kilometers and b_1 , b_2 , and b_3 are adjustable constants. The arbitrary constant 25 that is added to the distance is for the purpose of reducing the predicted values at small distances. The size of the constant has a very large influence on the values at small distances, but sufficient data points at these distances are not available for a meaningful determination of the appropriate size. Donovan states that the function fits the data better when the arbitrary constant is 25 than when it is zero, but it is unclear why it should be 25 rather than 15, 10, or 5.

The corresponding curves are compared in figure 48 for a magnitude 7.6 earthquake. The solid lines show the 70 percent prediction interval for the magnitude 7.1-7.6 data set of this report. Most of the points in that data

set came from the magnitude 7.2 Kern County earthquake. The apparent inconsistency in comparing curves for a magnitude 7.6 earthquake with data from a magnitude 7.2 event is connected with the various magnitudes that can be given one earthquake. At the time that the relations shown in figure 48 were developed, the only available magnitude for the Kern County earthquake was 7.7, based on surface wave data; it was not until 1978 that the Richter local magnitude of 7.2 was published. It should be noted that the

commonly used magnitudes will saturate as the size of the earthquake increases. A number of recent papers have discussed this important point; see, e.g., Brune (1970), Geller (1976), Kanamori (1977), and Hanks and Kanamori (1978).

The amount of disagreement shown in figures 47 and 48 is not surprising in view of the different assumptions, different measures of distance, and different data sets used in arriving at the different curves. The disagreement is, as might be expected, the greatest at short distances.

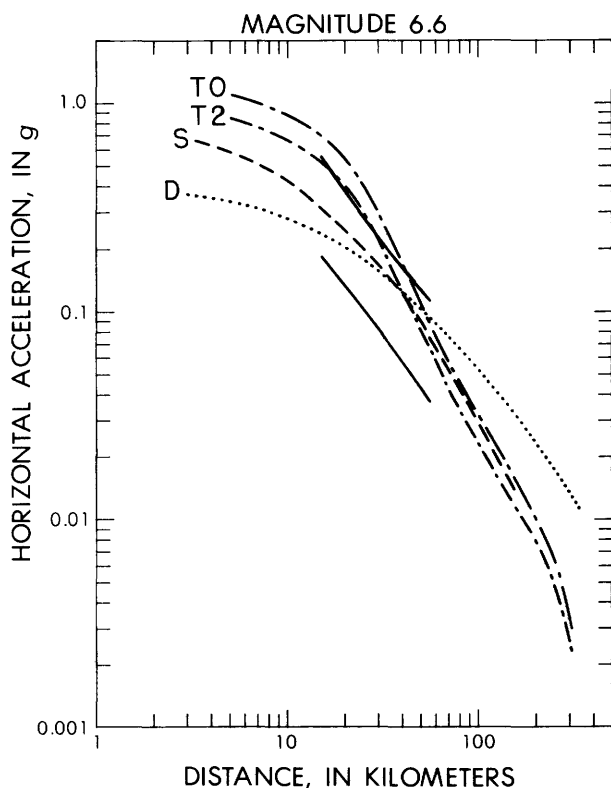


Figure 47. Proposed relations of peak horizontal acceleration to distance from slipped fault for magnitude 6.6 earthquake. Curve labeled S is given by Schnabel and Seed (1973) for rock sites, curve labeled D is given by Donovan (1973) for soil sites, and curves labeled T0 and T2 are mean curves given by Trifunac (1976) for soft and hard sites, respectively. Solid lines show 70 percent prediction interval for data set for magnitude class 6.0-6.4 and small structures, from this report.

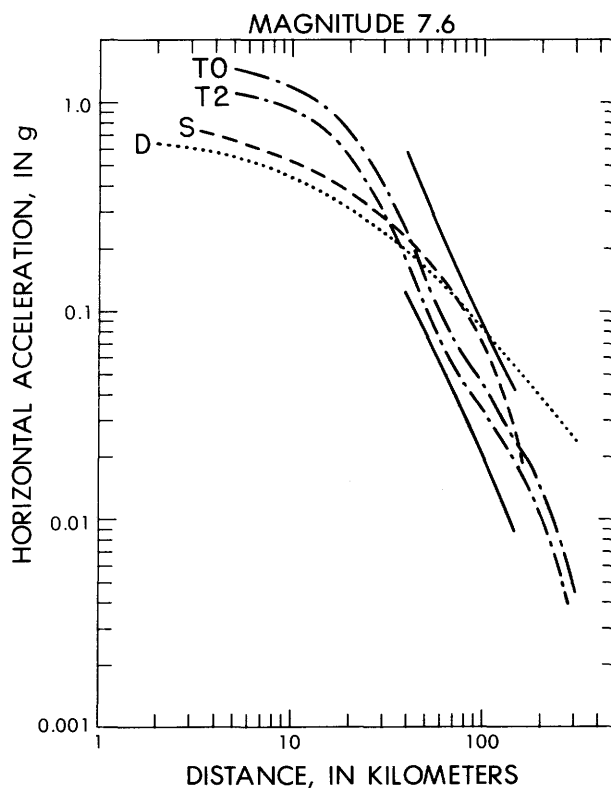


Figure 48. Proposed relations of peak horizontal acceleration to distance from slipped fault for magnitude 7.6 earthquake. Curves labeled S, D, T0 and T2 are from sources given in figure 47. Solid lines show 70 percent prediction interval for data set for magnitude class 7.1-7.6 and small structures, from this report.

ESTIMATION OF PEAK PARAMETERS AT SHORT DISTANCES

The regression lines given in a preceding section of this report provide the means for estimating peak ground motion parameters at distances greater than 5 km for magnitude 5.0-5.7 earthquakes, at distances greater than 15 km for magnitude 6.0-6.4 earthquakes, and at distances greater than 40 km for magnitude 7.1-7.6 earthquakes. Unfortunately, most of the damage from earthquakes can be expected to occur at shorter distances. Attempts have been made, as described in the preceding section, to provide curves for estimating at shorter distances. For reasons given in that section, we do not have complete confidence in those curves. We will not venture our own set of curves but will discuss briefly some of the considerations bearing on ground-motion estimates near the source. Further discussions of these questions in greater depth is given by Boore (1974).

Several studies have used simplified models of the faulting process to set limits on the ground motion at the fault surface (Housner, 1965; Ambraseys, 1969; Brune, 1970; Ida, 1973). Brune's (1970) near-source model assumes that rupture occurs instantaneously over the fault plane. The peak particle velocity is proportional to the stress drop and equals 100 cm/s for a stress drop of 10 MPa (100 bars). The peak acceleration is infinite if all frequencies are included, but if frequencies above 10 Hz are filtered out of the acceleration pulse the peak value is $2g$. This is a useful model for relating ground motion to the physics of the rupture process, but it does not give firm upper limits. An argument can be made for larger motions if one takes rupture propagation into account (Ida, 1973; Andrews, 1976). Furthermore, the peak values of ground motion may represent localized high stress drops, as Hanks and Johnson (1976) have suggested for peak acceleration. Such localized stress drops might easily exceed 100 MPa.

The peak acceleration at the surface is limited by the strength of near-surface materials, as has been pointed out by Ambraseys (1974). For sites near the source underlain by soil material of low strength, this factor may control the value of peak acceleration. This consideration may also apply to rock sites if the rock is sufficiently weathered. Determination of the limiting acceleration, however, would require reliable measurement of the dynamic, *in situ* strength of the soil at a particular site. In the absence of adequate measurements, one must presume that the acceleration could be at least as large as $0.5g$, which was recorded on a thickness of more than 60 m of

water-saturated alluvium at station 2 in the Parkfield earthquake (Shannon and Wilson, Inc. and Agabian Associates, 1976).

For displacement, it seems unlikely that the peak would exceed the static dislocation amplitude. The latter is known for many historical earthquakes and may be estimated as a function of magnitude (Bonilla and Buchanan, 1970).

The accelerogram recorded at Pacoima Dam during the San Fernando earthquake has major significance for estimates of near-source ground motion. The instrument is located only 3 km from the rupture surface at a rock site where the topographic relief is severe. The peak recorded horizontal acceleration is $1.25g$, velocity 113 cm/s, and displacement 38 cm. This is the only accelerogram in the data set recorded within 5 km for an earthquake of magnitude as large as 6.4, and as such ought to have strong influence on estimates of near-source ground motion. The possibility of topographic amplification needs consideration. A two-dimensional finite-difference study by Boore (1973) suggests that the acceleration may have been amplified by as much as 50 percent but that the velocity and displacement were relatively unaffected. Given these considerations, it would be difficult for us to accept estimates less than about $0.8g$, 110 cm/s, and 40 cm, respectively, for the mean values of peak acceleration, velocity and displacement at rock sites within 5 km of fault rupture in a magnitude 6.5 earthquake. We recognize that these numbers represent one earthquake with a particular focal mechanism and that estimates can be expected to change when more data become available. We presume that the statistical scatter about the mean will be at least as great for sites close to the rupture as at the greater distances where data are available.

The accelerograph at Pacoima dam was only 3 km from the nearest point on the rupture surface, but the nearest point was not the source of the peak motions. As noted previously the source for the peak velocity and for the peak acceleration are different points on the rupture surface separated by perhaps as much as 20 km (Hanks, 1974; Bouchon and Aki, 1977).

Above magnitude 6.5 there are essentially no data for estimating the effect of magnitude on near-fault peak acceleration, velocity and displacement, other than the static fault offset as a bound on the peak displacement. Conservatism requires the presumption of some increase with magnitude. Hanks and Johnson (1976) presented a set of peak acceleration data at a source distance of approximately 10 km for earthquakes in the magnitude range 3.2-7.1. The only data point above magnitude 6.5 was for the Imperial Valley earthquake of 1940 which they assign a magnitude of 7.1 in

contrast to our value 6.4, so the data set can be applied to magnitudes greater than 6.5 only as an extrapolation. The data set shows some dependence of peak accelerations on magnitude, but Hanks and Johnson argue that the data are consistent with the idea of magnitude-independent source properties. The data plotted as the logarithm of peak acceleration against magnitude can be fit by a straight line with a slope equivalent to an increase by a factor of 1.4 per magnitude unit. This should not be used for extrapolation beyond magnitude 6.5, however, because the data set was deliberately chosen to represent relatively high values, and thus the slope of the line fitting the data may not be the same as the slope of the line representing mean values or, for that matter, of the line representing values for any fixed probability.

At sites other than rock sites accelerations might be less because of the limited strength of near-surface materials, but, as previously noted, determining how much less would require dynamic, *in situ* measurements of soil properties. The amplification of peak velocity at soil sites compared to rock sites may not be so great close to the fault because of the energy lost in nonlinear soil deformation, but numerical modeling (Joyner and Chen, 1975) demonstrates the possibility of amplification of velocity by as much as 30 percent even under conditions of intense deformation. The possibility of greater amplification cannot be excluded. Amplification of displacement at soil sites should be expected close to the fault, as at greater distances, if the soil column is sufficiently thick.

REFERENCES CITED

- Acton, F. S., 1959, Analysis of straight-line data: New York, Dover, 267 p.
- Allen, C. R., Engen, G. R., Hanks, T. C., Nordquist, J. M., and Thatcher, W. R., 1971, Main shock and larger aftershocks of the San Fernando earthquake, February 9 through March 1, 1971, *in* The San Fernando, California, earthquake of February 9, 1971: U. S. Geological Survey Professional Paper 733, p. 17-20.
- Allen, C. R., Hanks, T. C., Whitcomb, J. H., 1973, San Fernando earthquake: Seismological studies and their tectonic implications, *in* San Fernando, California, earthquake of February 9, 1971, v. 3: National Oceanic and Atmospheric Administration, U. S. Department of Commerce, p. 13-21.
- Allen, C. R., and Nordquist, J. M., 1972, Fore-shock, main shock, and larger aftershocks of the Borrego Mountain earthquake, *in* The Borrego Mountain earthquake of April 9, 1968: U.S. Geological Survey Professional Paper 787, p. 16-23.
- Ambraseys, N. N., 1969, Maximum intensity of ground movements caused by faulting: World Conference on Earthquake Engineering, 4th, Santiago, Chile, Proceedings, v. 1, p. A2-154-A2-171.
- Ambraseys, N. N., 1974, Dynamics and response of foundation materials in epicentral regions of strong earthquakes: World Conference on Earthquake Engineering, 5th, Rome, Italy, 1973, Proceedings, v. 1, p. CXXVI-CXLVIII.
- Andrews, D. J., 1976, Rupture propagation with finite stress in antiplane strain: *Journal of Geophysical Research*, v. 81, p. 3575-3582.
- Arnold, Peter, Vanmarcke, E. H., and Gazetas, George, 1976, Frequency content of ground motions during the 1971 San Fernando earthquake: Massachusetts Institute of Technology, Department of Civil Engineering, Publication R76-3, 73 p.
- Bolt, B. A., 1978, The local magnitude M_L of the Kern County earthquake of July 21, 1952: *Seismological Society of America Bulletin*, v. 68, p. 513-515.
- Bonilla, M. G., and Buchanan, J. M., 1970, Interim report on worldwide historic surface faulting: U.S. Geological Survey Open-File Report, 32 p.

- Boore, D. M., 1973, The effect of simple topography on seismic waves: implications for the accelerations recorded at Pacoima Dam, San Fernando Valley, California: Seismological Society of America Bulletin, v. 63, p. 1603-1609.
- Boore, D. M., 1974, Empirical and theoretical study of near-fault wave propagation: World Conference on Earthquake Engineering, 5th, Rome, Italy, 1973, Proceedings, v. 2, p. 2397-2408.
- Boore, D. M., and Stierman, D. J., 1976, Source parameters of the Pt. Mugu, California, earthquake of February 21, 1973: Seismological Society of America Bulletin, v. 66, p. 385-404.
- Bouchon, M., and Aki, K., 1977, Discrete wave-number representation of seismic-source wave fields: Seismological Society of America Bulletin, v. 67, p. 259-277.
- Brune, J. N., 1970, Tectonic stress and the spectra of seismic shear waves from earthquakes: Journal of Geophysical Research, v. 75, p. 4997-5009.
- Bufe, C. G., Lester, F. W., Lahr, K. M., Lahr, J. C., Seekins, L. C., and Hanks, T. C., 1976, Oroville earthquakes: normal faulting in the Sierra Nevada foothills: Science, v. 192, p. 72-74.
- Cloud, W. K., 1959, Intensity and ground motion of the San Francisco earthquake of March 22, 1957, in San Francisco earthquakes of March 1957: California Division of Mines Special Report 57, p. 49-57.
- Cloud, W. K., and Knudson, C. F., no date, Preliminary engineering seismological report, in The Fairbanks, Alaska, earthquake of June 21, 1967: Coast and Geodetic Survey, U.S. Department of Commerce, p. 33-60.
- Cloud, W. K., and Perez, Virgilio, 1967, Accelerograms - Parkfield earthquake: Seismological Society of America Bulletin, v. 57, p. 1179-1192.
- Crouse, C. B., and Jennings, P. C., 1975, Soil-structure interaction during the San Fernando earthquake: Seismological Society of America Bulletin, v. 65, p. 13-36.
- Dewey, J. W., Algermissen, S. T., Langer, C., Dillinger, W., and Hopper, M., 1973, The Managua earthquake of 23 December 1972: Location, focal mechanism, aftershocks, and relationship to recent seismicity of Nicaragua, in Managua, Nicaragua earthquake of December 23, 1972: Earthquake Engineering Research Institute Conference, Proceedings, v. 1, p. 66-88.
- Dixon, W. J., and Massey, F. J., Jr., 1957, Introduction to statistical analyses: New York, McGraw-Hill, 488 p.
- Donovan, N. C., 1973, A statistical evaluation of strong motion data including the February 9, 1971 San Fernando earthquake: World Conference on Earthquake Engineering, 5th, Rome, Italy, Proceedings, v. 1, p. 1252-1261.
- Duke, C. M., Johnsen, K. E., Larson, L. E., and Engman, D. C., 1972, Effects of site classification and distance on instrumental indices in the San Fernando earthquake: University of California, Los Angeles, School of Engineering and Applied Science, UCLA-ENG-7247, 29 p.
- Duke, C. M., Luco, J. E., Carriveau, A. R., Hradilek, P. J., Lastrico, R., and Ostrom, D., 1970, Strong earthquake motion and site conditions, Hollywood: Seismological Society of America Bulletin, v. 60, p. 1271-1289.
- Earthquake Engineering Research Laboratory, 1969-1975, Strong-motion earthquake accelerograms, v. 1, Parts A-Y, v. 2, Parts A-Y: California Institute of Technology, Earthquake Engineering Research Laboratory.
- Ellsworth, W. L., 1975, Bear Valley, California, earthquake sequence of February-March 1972: Seismological Society of America Bulletin, v. 65, p. 483-506.
- Ellsworth, W. L., Campbell, R. H., Hill, D. P., Page, R. A., Alewine, R. W., III, Hanks, T. C., Heaton, T. H., Hileman, J. A., Kanamori, H., Minster, B., and Whitcomb, J. H., 1973, Point Mugu, California, earthquake of 21 February 1973 and its aftershocks: Science, v. 182, p. 1127-1129.
- Gedney, Larry, and Berg, Edward, 1969, The Fairbanks earthquakes of June 21, 1967; aftershock distribution, focal mechanisms, and crustal parameters: Seismological Society of America Bulletin, v. 59, p. 73-100.
- Geller, R. J., 1976, Scaling relations for earthquake source parameters and magnitudes, Seismological Society of America Bulletin, v. 66, p. 1501-1523.
- Hamilton, R. M., 1972, Aftershocks of the Borrego Mountain earthquake from April 12 to June 12, 1968, in The Borrego Mountain earthquake of April 9, 1968: U.S. Geological Survey Professional Paper 787, p. 31-54.
- Hanks, T. C., 1974, The faulting mechanism of the San Fernando earthquake: Journal of Geophysical Research, v. 79, p. 1215-1229.

- Hanks, T. C., 1975, Strong ground motion of the San Fernando, California earthquake, ground displacements: Seismological Society of America Bulletin, v. 65, p. 193-225.
- Hanks, T. C., and Johnson, D. A., 1976, Geophysical assessment of peak accelerations: Seismological Society of America Bulletin, v. 66, p. 959-968.
- Hanks, T. C., and Kanamori, H., 1978, A note on moment-magnitude scales, Journal of Geophysical Research (submitted).
- Housner, G. W., 1965, Intensity of earthquake ground shaking near the causative fault: World Conference on Earthquake Engineering, 3rd, Wellington, New Zealand, Proceedings, v. 1, p. III-94-III-109.
- Ida, Yoshiaki, 1973, The maximum acceleration of seismic ground motion: Seismological Society of America Bulletin, v. 63, p. 959-968.
- Jennings, C. W., and Strand, R. G., 1959, Geologic map of California, Santa Cruz sheet, scale 1:250,000: California Division of Mines and Geology.
- Jennings, C. W., and Strand, R. G., 1969, Geologic map of California, Los Angeles sheet, scale 1:250,000: California Division of Mines and Geology.
- Joyner, W. B., and Chen, A. T. F., 1975, Calculation of nonlinear ground response in earthquakes: Seismological Society of America Bulletin, v. 65, p. 1315-1336.
- Kanamori, H., 1977, The energy release in great earthquakes, Journal of Geophysical Research, v. 82, p. 2981-2987.
- Kanamori, H., and Jennings, P. C., 1978, Determination of local magnitude, M_L , from strong-motion accelerograms: Seismological Society of America Bulletin, v. 68, p. 471-485.
- Knudson, C. F., and Hansen A., Francisco, 1973, Accelerograph and seismoscope records from Managua, Nicaragua, earthquakes, *in* Managua, Nicaragua earthquake of December 23, 1972: Earthquake Engineering Research Institute Conference, Proceedings, v. 1, p. 180-205.
- Lahr, K. M., Lahr, J. C., Lindh, A. G., Bufe, C. G., and Lester, F. W., 1976, The August 1975 Oroville earthquakes: Seismological Society of America Bulletin, v. 66, p. 1085-1099.
- Lindh, A. G., and Boore, D. M., 1973, Another look at the Parkfield earthquake, using strong motion instruments as a seismic array (abs.): Seismological Society of America, Earthquake Notes, v. 44, p. 24.
- Maley, R. P., and Cloud, W. K., 1973, Strong-motion accelerograph records, *in* San Fernando, California, earthquake of February 9, 1971, v. 3: National Oceanic and Atmospheric Administration, U.S. Department of Commerce, p. 325-348.
- Maley, R. P., Perez, Virgilio, and Morrill, B. J., 1975, Strong-motion seismograph results from the Oroville earthquake of 1 August 1975, *in* Oroville, California, earthquake 1 August 1975: California Division of Mines and Geology Special Report 124, p. 115-122.
- McEvelly, T. V., Bakun, W. H., and Casaday, K. B., 1967, The Parkfield, California, earthquakes of 1966: Seismological Society of America Bulletin, v. 57, p. 1221-1244.
- Nason, Robert, Harp, E. L., La Gesse, Harry, and Maley, R. P., 1975, Investigations of the 7 June 1975 earthquake in Humboldt County, California: U.S. Geological Survey Open-File Report 75-404, 28 p.
- Newmark, N. M., Blume, J. A., and Kapur, K. K., 1973, Seismic design spectra for nuclear power plants: American Society of Civil Engineers Proceedings, Journal of Power Division, v. 99, p. 287-303.
- Newmark, N. M., and Hall, W. J., 1969, Seismic design criteria for nuclear reactor facilities: World Conference Earthquake Engineering, 4th, Santiago, Chile, Proceedings, v. 2, p. B4-37-B4-50.
- Nuttli, O. W., 1952, The Western Washington earthquake of April 13, 1949: Seismological Society of America Bulletin, v. 42, p. 21-28.
- Page, R. A., Boore, D. M., Joyner, W. B., and Coulter, H. W., 1972, Ground Motion values for use in the seismic design of the trans-Alaska pipeline system: U.S. Geological Survey Circular 672, 23 p.
- Page, R. A., Boore, D. M., and Dieterich, J. H., 1975, Estimation of bedrock motion at the ground surface, *in* R. D. Borcherdt, ed., Studies for seismic zonation of the San Francisco Bay region: U.S. Geological Survey Professional Paper 941-A, p. A31-A38.
- Page, R. A., and Gawthrop, W., 1973, The Sitka, Alaska, earthquake of 30 July 1972 and its aftershocks (abs.): Seismological Society of America, Earthquake Notes, v. 44, p. 16-17.
- Person, W. J. (ed.), 1975, Seismological notes-- November-December 1974: Seismological Society of America Bulletin, v. 65, p. 1035-1038.
- Richter, C. F., 1955, Foreshocks and aftershocks, *in* Earthquakes in Kern County California during 1952: California Division of Mines Bulletin, 171, p. 171-175.

- Richter, C. F., 1958, Elementary seismology: San Francisco, W. H. Freeman, 768 p.
- Schnabel, P. B., and Seed, H. B., 1973, Accelerations in rock for earthquakes in the western United States: Seismological Society of America Bulletin, v. 63, p. 501-516.
- Seed, H. B., Murarka, R., Lysmer, J., and Idriss, I. M., 1976, Relationships of maximum acceleration, maximum velocity, distance from source, and local site conditions for moderately strong earthquakes: Seismological Society of America Bulletin, v. 66, p. 1323-1342.
- Shannon and Wilson, Inc., and Agabian Associates, 1976, Geotechnical and strong motion earthquake data from U.S. accelerograph stations Ferndale, Cholame, and El Centro, California, Volume I: NUREG-0029 Vol. 1 NRC-6, Clearinghouse, Springfield, VA 22151.
- Steinbrugge, K. V., Cloud, W. K., and Scott, N. H., 1970, The Santa Rosa, California, earthquakes of October 1, 1969; U.S. Department of Commerce, 99 p.
- Stierman, D. J., and Ellsworth, W. L., 1976, Aftershocks of the February 21, 1973 Point Mugu, California earthquake: Seismological Society of America Bulletin, v. 66, p. 1931-1952.
- Tocher, Don, 1959, Seismographic results from the 1957 San Francisco earthquakes, *in* San Francisco earthquakes of March 1957: California Division of Mines Special Report, p. 59-71.
- Tocher, Don, 1962, The Hebgen Lake, Montana, earthquake of August 17, 1959, MST: Seismological Society of America Bulletin, v. 52, p. 153-162.
- Trifunac, M. D., 1972, Tectonic stress and the source mechanism of the Imperial Valley, California, earthquake of 1940: Seismological Society of America Bulletin, v. 62, p. 1283-1302.
- Trifunac, M. D., 1976, Preliminary analysis of the peaks of strong earthquake ground motion -- dependence of peaks on earthquake magnitude, epicentral distance, and recording site conditions: Seismological Society of America Bulletin, v. 66, p. 189-219.
- Trifunac, M. D., and Brady, A. G., 1975, On the correlation of seismic intensity scales with the peaks of recorded strong ground motion: Seismological Society of America Bulletin, v. 65, p. 139-162.
- Trifunac, M. D., and Brady, A. G., 1976, Correlations of peak acceleration, velocity, and displacement with earthquake magnitude, distance, and site conditions: Earthquake Engineering and Structural Dynamics, v. 4, p. 455-471.
- Trifunac, M. D., and Brune, J. N., 1970, Complexity of energy release during the Imperial Valley, California earthquake of 1940: Seismological Society of America Bulletin, v. 60, p. 137-160.
- Trifunac, M. D., and Udwadia, F. E., 1974, Parkfield, California, earthquake of June 27, 1966: a three-dimensional moving dislocation: Seismological Society of America Bulletin, v. 64, p. 511-533.
- Unger, J. D., and Eaton, J. P., 1970, Aftershocks of the October 1, 1969, Santa Rosa, California, earthquakes: Geological Society of America Abstracts with Programs, v. 2, p. 155.
- U.S. Coast and Geodetic Survey and Earthquake Engineering Research Laboratory, 1968, Strong-motion instrumental data on the Borrego Mountain earthquake of 9 April 1968: U.S. Coast and Geodetic Survey, Earthquake Engineering Research Laboratory, California Institute of Technology, 119 p.
- U.S. Dept. of Commerce, serial publication, U.S. Earthquakes.
- U.S. Geol. Survey, 1974, Seismic engineering program report, October-December 1974: U.S. Geological Survey Circular, 713, 19 p.
- U.S. Geol. Survey, 1975, Seismic engineering program report, January-March 1975: U.S. Geological Survey circular 717-A, 17 p.
- U.S. Geol. Survey, 1976a, Seismic engineering program report, July-September 1975: U.S. Geological Survey circular 717-C, 17 p.
- U.S. Geol. Survey, 1976b, Strong-motion accelerograph station list--1975: U.S. Geological Survey Open-File Report, 76-79, 81 p.
- Valera, J. E., 1973, Soil conditions and local soil effects during the Managua earthquake of December 23, 1972, *in* Managua, Nicaragua earthquake of December 23, 1972: Earthquake Engineering Research Institute Conference, Proceedings, v. 1, p. 232-264.
- Ward, P. L., Harlow, David, Gibbs, James, and Aburto Q., Arturo, 1973, Location of the main fault that slipped during the Managua earthquake as determined from locations of some aftershocks, *in* Managua, Nicaragua earthquake of December 23, 1972: Earthquake Engineering Research Institute Conference, Proceedings, v. 1, p. 89-96.

STATISTICAL PARAMETERS

Linear regression analysis (Dixon and Massey, 1957) was employed to describe the distance dependence of the peak parameters. Using the symbol y for the peak parameter and the symbol x for distance we fit the data by a straight line

$$v = A + B u$$

where $v = \log_{10} y$

and $u = \log_{10} x$.

Values for A and B are given by the following equations

$$A = \frac{\sum v - B \sum u}{n}$$

$$B = \frac{n \sum uv - \sum u \sum v}{n \sum u^2 - (\sum u)^2}$$

where the summations are taken over all the points in the data set and n is the number of points. The scatter in the data is measured by $s_{v|u}$, the standard error of estimate of v for a given u . That quantity is obtained from the following equations:

$$s_{v|u} = \frac{n-1}{n-2} (s_v^2 - B s_u^2)$$

$$s_u^2 = \frac{1}{n(n-1)} [n \sum u^2 - (\sum u)^2]$$

$$s_v^2 = \frac{1}{n(n-1)} [n \sum v^2 - (\sum v)^2].$$

For a given confidence level, the prediction interval for a single prediction of v given u is

$$(A + Bu) \pm t_{\alpha/2, n-2} s_{v|u} \sqrt{1 + \frac{1}{n} + \frac{(u - \bar{u})^2}{(n-1) s_u^2}}$$

where \bar{u} is the mean of u values, the confidence level is $(1 - \alpha)$, and $t_{\alpha/2, n-2}$ is the abscissa of the Student's t distribution for a cumulative probability of $(1 - \alpha/2)$ and $(n - 2)$ degrees of freedom. The lines describing the prediction intervals are curved because of statistical uncertainty in the regression coefficient B . A measure of that uncertainty is the standard error of B , which is given by

$$s_B = \frac{s_{v|u}}{s_u \sqrt{n-1}}$$

The following table lists the statistical parameters A , B , $s_{v|u}$, s_B and n for the data sets discussed in the text. The number of the figure displaying the data set is also given.

Data set	Fig. No.	A	B	$s_{v u}$	s_B	n
Horizontal acceleration						
M = 5.0-5.7 class 1-----	1	0.17	-0.93	0.37	0.46	19
M = 6.0-6.4 class 1-----	2	.96	-1.23	.20	.32	16
M = 7.1-7.6 class 1-----	3	2.65	-2.01	.26	.43	9
M = 5.0-5.7 all-----	23	.05	-.86	.35	.40	24
M = 6.0-6.4 all-----	24	.81	-1.20	.20	.15	44
M = 7.1-7.6 all-----	25	2.65	-2.00	.21	.31	14
San Fernando R1-----	39	1.45	-1.56	.18	.23	10
San Fernando S1-----	39	1.09	-1.34	.18	.25	12
San Fernando S2-----	33	.90	-1.29	.15	.15	18
Horizontal velocity						
M = 5.3-5.7 class 1-----	5	2.35	-1.22	.38	.61	11
M = 6.4 class 1-----	6	1.93	-.58	.25	.45	14
M = 7.1-7.2 class 1-----	7	2.45	-.72	.16	.42	6
M = 5.3-5.7 all-----	26	2.31	-1.26	.35	.48	16
M = 6.4 all-----	27	2.35	-.85	.20	.19	35
San Fernando R1-----	41	3.12	-1.51	.26	.39	9
San Fernando S1-----	41	3.06	-1.31	.16	.23	11
San Fernando S2-----	35	2.60	-.96	.08	.08	18
Horizontal displacement						
M = 5.3-5.7 class 1-----	9	1.81	-1.15	.36	.59	11
M = 6.4 class 1-----	10	1.48	-.55	.30	.53	14
M = 7.1-7.2 class 1-----	11	2.34	-.86	.22	.56	6
M = 5.3-5.7 all-----	29	1.60	-1.03	.34	.46	16
M = 6.4 all-----	30	1.91	-.77	.28	.27	35
San Fernando R1-----	43	2.72	-1.52	.25	.38	9
San Fernando S1-----	43	2.07	-.90	.25	.37	11
San Fernando S2-----	37	2.09	-.76	.19	.18	18
Vertical acceleration						
M = 5.0-5.7 class 1-----	14	-.27	-.77	.29	.36	19
M = 6.0-6.4 class 1-----	15	1.36	-1.70	.20	.32	16
M = 7.1-7.6 class 1-----	16	1.55	-1.58	.21	.39	8
Vertical velocity						
M = 5.3-5.7 class 1-----	17	1.62	-.96	.30	.48	11
M = 6.4 class 1-----	18	1.86	-.80	.18	.32	14
Vertical displacement						
M = 5.3-5.7 class 1-----	20	1.22	-.93	.29	.47	11
M = 6.4 class 1-----	21	1.15	-.53	.14	.25	14

STRONG-MOTION DATA

Associated with each earthquake is a six-digit number followed by a four-digit number. The first two digits of the six-digit number denote the year, the second two the month, and the third two the day. The first two digits of the four-digit number represent the hour (Universal Time) and the second two the minute.

Explanation of abbreviations:

- MAG** - Earthquake Magnitude. Richter (1958) local magnitude if available, otherwise surface wave magnitude, except for the 1949 Puget Sound and 1959 Hebgen Lake events, for which the type of magnitude was not specified in the literature.
- STA #** - Station number as given by the U.S. Geological Survey (1976b).
- STRUC** - Code for associated structure. One if data were recorded at the base of a one- or two-story building, two if data were recorded at the base of a larger building or on a dam abutment.
- DIST** - Shortest distance in km to the surface of fault slippage.
- AC** - Accuracy code for distance. A if the uncertainty is less than 2 km, B if it is between 2 and 5 km, and C if it is between 5 and 25 km.
- ACCEL** - Peak acceleration as a fraction of the acceleration of gravity.
- VEL** - Peak velocity in centimeters per second.
- DISP** - Peak displacement in centimeters.
- DUR** - Duration in seconds, defined as the time interval between the first and last horizontal acceleration peaks equal to or greater than 0.05 g.
- SRC** - Code denoting source of strong motion data. List is given following the data.
- GEO** - Code for geologic conditions at recording site. S for soil (thicker than 4 to 5 meters) and R for rock.
- REF** - Code for source of information on stations. List of references follows station list.
- *** - Denotes station selected from the special area in downtown Los Angeles as described in the text.

LISTING OF STRONG MOTION DATA

720224 1556 BEAR VALLEY, CALIFORNIA

MAG = 5.0

SOIL STATIONS:		***** HORIZONTAL *****										***** VERTICAL *****			STATION LOCATION
STA#	STRUC	DIST	AC	ACCEL	VEL	DISP	DUR	SRC	ACCEL	VEL	DISP	SRC			
1028	1	31.0	A	0.030				B	0.010			B	HOLLISTER - CITY HALL		

741128 2301 BEAR VALLEY, CALIFORNIA

MAG = 5.2

ROCK STATIONS:		***** HORIZONTAL *****										***** VERTICAL *****			STATION LOCATION
STA#	STRUC	DIST	AC	ACCEL	VEL	DISP	DUR	SRC	ACCEL	VEL	DISP	SRC			
1032	1	18.0	A	0.011				E	0.013			E	SAGO CENTRAL - HARRIS RANCH		

SOIL STATIONS:		***** HORIZONTAL *****										***** VERTICAL *****			STATION LOCATION
STA#	STRUC	DIST	AC	ACCEL	VEL	DISP	DUR	SRC	ACCEL	VEL	DISP	SRC			
1377	1	8.9	A	0.120				G	0.050			G	SAN JUAN BAUTISTA (C126) - 24 POLK		
1028	1	10.8	A	0.170				G	0.070			G	HOLLISTER - CITY HALL		
1250	1	10.8	A	0.140				G	0.030			G	GILROY (C6) - GEOL BLDG, GAL COL		
1202	1	37.0	A	0.030				G	0.050			G	STONE CANYON EAST, CALIF.		

750607 846 FERNDALE, CALIFORNIA

MAG = 5.2

ROCK STATIONS:		***** HORIZONTAL *****										***** VERTICAL *****			STATION LOCATION
STA#	STRUC	DIST	AC	ACCEL	VEL	DISP	DUR	SRC	ACCEL	VEL	DISP	SRC			
1249	1	32.0	B	0.220				I	0.030			I	CAPE MENDOCINO (C5) - PETROLIA		
1278	1	64.0	B	0.100				I					SHELTER COVE, STA 2 (C41) - PWR PLT		

SOIL STATIONS:		***** HORIZONTAL *****										***** VERTICAL *****			STATION LOCATION
STA#	STRUC	DIST	AC	ACCEL	VEL	DISP	DUR	SRC	ACCEL	VEL	DISP	SRC			
1023	1	24.0	B	0.240				I	0.050			I	FERNDALE - OLD CITY HALL, BROWN ST		
1398	1	34.0	B	0.190				I	0.030			I	PETROLIA (C156) - GENERAL STORE		

570322 1944 DALY CITY, CALIFORNIA

MAG = 5.3

ROCK STATIONS:		***** HORIZONTAL *****										***** VERTICAL *****			STATION LOCATION
STA#	STRUC	DIST	AC	ACCEL	VEL	DISP	DUR	SRC	ACCEL	VEL	DISP	SRC			
1117	1	8.0	B	0.127	4.9	2.3	1.6	A	0.051	1.2	0.7	A	SAN FRANCISCO - GOLDEN GATE PARK		

SOIL STATIONS:		***** HORIZONTAL *****										***** VERTICAL *****			STATION LOCATION
STA#	STRUC	DIST	AC	ACCEL	VEL	DISP	DUR	SRC	ACCEL	VEL	DISP	SRC			
1080	2	12.0	B	0.103	5.0	1.1	1.4	A	0.050	2.3	0.6	A	SAN FRANCISCO - STATE BLDG		
1065	2	14.0	B	0.055	2.9	1.3	0.0	A	0.036	1.3	0.4	A	SAN FRANCISCO - ALEXANDER BLDG		
1078	2	14.0	B	0.048	5.0	1.4	0.0	A	0.034	1.5	0.9	A	SAN FRANCISCO - SOUTHERN PACIFIC BG		
1049	2	24.0	B	0.047	1.9	1.5	0.0	A	0.023	0.9	1.3	A	OAKLAND - CITY HALL		
1081	2	58.0	B	0.007				R	0.005			B	SAN JOSE - BANK OF AMERICA BLDG		

700912 1430 LYTLE CREEK, CALIFORNIA

MAG = 5.4

ROCK STATIONS:		***** HORIZONTAL *****								***** VERTICAL *****				STATION LOCATION
STA#	STRUC	DIST	AC	ACCEL	VEL	DISP	DUR	SRC	ACCEL	VEL	DISP	SRC		
290	1	15.0	B	0.205	9.6	2.2	2.8	A	0.076	3.2	1.4	A	WRIGHTWOOD - 6074 PARK DRIVE	
111	1	18.0	B	0.086	5.5	2.4	1.1	A	0.093	2.6	1.2	A	CEDAR SPRINGS - ALLEN RANCH	
116	1	19.0	B	0.179				A	0.094			A	DEVILS CANYON - FILTER PLANT	
278	2	32.0	B	0.022				A	0.018			A	SAN DIMAS - PUDDINGSTONE RESERVOIR	
104	2	46.0	B	0.054				A	0.016			A	ARCADIA - SANTA ANITA RESERVOIR	
266	1	58.0	B	0.015				B	0.010			B	PASADENA - CIT SEISMOLOGY LAB	
137	2	70.0	B	0.015				A	0.006			A	*LOS ANGELES - WATER & POWER	
110	1	110.0	B	0.025				A	0.011			A	CASTAIC - OLD RIDGE ROUTE	

SOIL STATIONS:		***** HORIZONTAL *****								***** VERTICAL *****				STATION LOCATION
STA#	STRUC	DIST	AC	ACCEL	VEL	DISP	DUR	SRC	ACCEL	VEL	DISP	SRC		
112	1	18.0	B	0.073	4.0	1.2	0.4	A	0.044	1.3	0.4	A	CEDAR SPRINGS - PUMP PLANT	
274	2	28.0	B	0.119	4.8	1.8	1.0	A	0.055	1.8	1.5	A	SAN BERNARDINO - HALL OF RECORDS	
113	1	29.0	B	0.045	2.5	0.9	0.0	A	0.042	1.3	0.7	A	COLTON - S. CAL. EDISON CO.	
129	2	34.0	B	0.019				B	0.009			B	LOMA LINDA - UNIV. MED. CENTER	
264	2	57.0	B	0.023	1.5	1.8	0.0	A	0.015	0.7	0.5	A	PASADENA - CIT MILLIKAN LIBRARY	
267	2	60.0	B	0.025	2.0	2.4	0.0	A	0.017	1.9	1.4	A	PASADENA - CIT JPL LAB	
181	2	66.0	B	0.026				A	0.012			A	LOS ANGELES - 1640 SOUTH MARENGO	
133	2	77.0	B	0.015				A	0.006			A	*HOLLYWOOD STORAGE - BASEMENT	
135	1	77.0	B	0.021				A	0.007			A	*HOLLYWOOD STORAGE - P.E. LOT	
125	1	95.0	B	0.010				A	0.006			A	LAKE HUGHES ARRAY 1 - FIRE STATION	
103	1	113.0	B	0.020				B	0.005			B	ANZA - ANZA POST OFFICE	

34

660628 426 PARKFIELD, CALIFORNIA

MAG = 5.5

ROCK STATIONS:		***** HORIZONTAL *****								***** VERTICAL *****				STATION LOCATION
STA#	STRUC	DIST	AC	ACCEL	VEL	DISP	DUR	SRC	ACCEL	VEL	DISP	SRC		
1438	1	16.1	A	0.411	22.5	5.5	3.7	A	0.165	4.4	1.4	A	CHOLAME-SHANDON: TEMPLOR	
1083	1	63.6	A	0.018	1.1	1.2	0.0	A	0.007	1.3	0.9	A	SAN LUIS OBISPO - CITY REC. BLDG	
110	1	204.0	A	0.004				B				B	CASTAIC - OLD RIDGE ROUTE	

SOIL STATIONS:		***** HORIZONTAL *****								***** VERTICAL *****				STATION LOCATION
STA#	STRUC	DIST	AC	ACCEL	VEL	DISP	DUR	SRC	ACCEL	VEL	DISP	SRC		
1013	1	6.6	A	0.509	78.1	26.4	12.1	A	0.349	14.1	4.3	A	CHOLAME-SHANDON ARRAY NO. 2	
1014	1	9.3	A	0.467	25.4	7.1	7.9	A	0.181	7.3	3.4	A	CHOLAME-SHANDON ARRAY NO. 5	
1015	1	13.0	A	0.279	11.8	4.4	7.8	A	0.138	4.5	2.1	A	CHOLAME-SHANDON ARRAY NO. 8	
1016	1	17.3	A	0.072	8.0	5.7	0.6	A	0.061	5.0	2.6	A	CHOLAME-SHANDON ARRAY NO. 12	
1095	1	105.0	A	0.012	2.2	2.5	0.0	A	0.007	1.1	1.5	A	TAFT - LINCOLN HS TUNNEL	
1011	1	112.0	A	0.006				B				B	BUENA VISTA - GROUND STATION	
1028	1	123.0	A	0.003				B				B	HOLLISTER - CITY HALL	
283	1	162.0	A	0.004				B	0.002			B	SANTA BARBARA - COURTHOUSE	
272	1	208.0	A	0.005				B	0.001			B	PORT HUENEME - NAVY LABORATORY	
133	2	261.0	A	0.001				B				B	*HOLLYWOOD STORAGE - BASEMENT	
135	1	261.0	A	0.001				B				B	*HOLLYWOOD STORAGE - P.E. LOT	
475	1	272.0	A	0.001				B				B	PASADENA - CIT ATHENAEUM	

670621 1804 FAIRBANKS, ALASKA

MAG = 5.6

ROCK STATIONS:

STA#	STRUC	DIST	AC	***** HORIZONTAL *****				***** VERTICAL *****				STATION LOCATION	
				ACCEL	VEL	DISP	DUR	SRC	ACCEL	VEL	DISP	SRC	
2707	1	15.0	B	0.060				C	0.060			C	FAIRBANKS, ALASKA - UNIV OF ALASKA

691002 456 SANTA ROSA, CALIFORNIA

MAG = 5.6

ROCK STATIONS:

STA#	STRUC	DIST	AC	***** HORIZONTAL *****				***** VERTICAL *****				STATION LOCATION	
				ACCEL	VEL	DISP	DUR	SRC	ACCEL	VEL	DISP	SRC	
1057	1	77.0	B	0.007				B	0.002			B	PLEASANT HILL - DIABLO VALLEY COL.
1074	2	79.0	B	0.011				R	0.004			B	SAN FRANCISCO - 390 MAIN

SOIL STATIONS:

STA#	STRUC	DIST	AC	***** HORIZONTAL *****				***** VERTICAL *****				STATION LOCATION	
				ACCEL	VEL	DISP	DUR	SRC	ACCEL	VEL	DISP	SRC	
1093	1	62.0	B	0.005				R	0.001			B	SAN PABLO - CONTRA COSTA COLLEGE
1065	2	79.0	B	0.008				R	0.003			B	SAN FRANCISCO - ALEXANDER BLDG
1071	2	79.0	B	0.015				R	0.007			B	SAN FRANCISCO - BETHLEHEM PAC BLDG
1078	2	79.0	B	0.016				R	0.007			B	SAN FRANCISCO - SOUTHERN PACIFIC BG
1049	2	82.0	B	0.006				R	0.002			B	OAKLAND - CITY HALL
1001	1	109.0	B	0.018				R	0.002			B	APEEL ARRAY - STATION 1
1002	1	110.0	B	0.017				R	0.002			B	APEEL ARRAY - STATION 2

691002 619 SANTA ROSA, CALIFORNIA

MAG = 5.7

ROCK STATIONS:

STA#	STRUC	DIST	AC	***** HORIZONTAL *****				***** VERTICAL *****				STATION LOCATION	
				ACCEL	VEL	DISP	DUR	SRC	ACCEL	VEL	DISP	SRC	
1057	1	77.0	B	0.009				R	0.002			B	PLFASANT HILL - DIABLO VALLEY COL.
1074	2	79.0	B	0.012				B	0.004			B	SAN FRANCISCO - 390 MAIN

SOIL STATIONS:

STA#	STRUC	DIST	AC	***** HORIZONTAL *****				***** VERTICAL *****				STATION LOCATION	
				ACCEL	VEL	DISP	DUR	SRC	ACCEL	VEL	DISP	SRC	
1093	1	62.0	B	0.003				R	0.003			B	SAN PABLO - CONTRA COSTA COLLEGE
1065	2	79.0	B	0.012				R	0.003			B	SAN FRANCISCO - ALEXANDER BLDG
1071	2	79.0	B	0.027				R	0.007			B	SAN FRANCISCO - BETHLEHEM PAC BLDG
1078	2	79.0	B	0.020				R	0.008			B	SAN FRANCISCO - SOUTHERN PACIFIC BG
1049	2	82.0	B	0.013				R	0.004			B	OAKLAND - CITY HALL
1001	1	109.0	B	0.029				R	0.002			B	APEEL ARRAY - STATION 1
1002	1	110.0	B	0.021				R	0.009			B	APEEL ARRAY - STATION 2

750801 2020 OROVILLE, CALIFORNIA

MAG = 5.7

ROCK STATIONS:		***** HORIZONTAL *****											***** VERTICAL *****			STATION LOCATION	
STA#	STRUC	DIST	AC	ACCEL	VEL	DISP	DUR	SRC	ACCEL	VEL	DISP	SRC	ACCEL	VEL	DISP	SRC	
1051	1	8.0	A	0.110	5.0	1.6	0.0	H	0.120	5.3	2.7	H					OROVILLE SEISMOGRAPH STATION
1293	1	32.0	A	0.040				H	0.030			H					PARADISE (C58) - KEWG TRNSMTR BLDG

SOIL STATIONS:		***** HORIZONTAL *****											***** VERTICAL *****			STATION LOCATION	
STA#	STRUC	DIST	AC	ACCEL	VEL	DISP	DUR	SRC	ACCEL	VEL	DISP	SRC	ACCEL	VEL	DISP	SRC	
1291	1	30.0	A	0.070				H	0.040			H					MARYSVILLE (C56) - CDOT MAINT BLDG
1292	1	31.0	A	0.080				H	0.030			H					CHICO (C57) - 2334 FAIR STREET

730221 1445 POINT MUGU, CALIFORNIA

MAG = 6.0

ROCK STATIONS:		***** HORIZONTAL *****											***** VERTICAL *****			STATION LOCATION	
STA#	STRUC	DIST	AC	ACCEL	VEL	DISP	DUR	SRC	ACCEL	VEL	DISP	SRC	ACCEL	VEL	DISP	SRC	
655	1	53.0	B	0.031				E	0.014			E					JENSEN FILTER PLT - 13100 BALBOA, LA

SOIL STATIONS:		***** HORIZONTAL *****											***** VERTICAL *****			STATION LOCATION	
STA#	STRUC	DIST	AC	ACCEL	VEL	DISP	DUR	SRC	ACCEL	VEL	DISP	SRC	ACCEL	VEL	DISP	SRC	
272	1	24.0	B	0.130				D	0.040			D					PORT HUENEME - NAVY LABORATORY
610	2	51.0	B	0.043				E	0.016			E					LOS ANGELES - 18321 VENTURA
657	2	51.0	B	0.036				E	0.012			E					SANTA MONICA - 201 OCEAN
118	2	53.0	B	0.042				E	0.016			E					LOS ANGELES - 16661 VENTURA
497	2	53.0	B	0.060				D	0.010			D					LOS ANGELES - 16633 VENTURA
512	2	54.0	B	0.036				F	0.016			E					LOS ANGELES - 16255 VENTURA
259	2	55.0	B	0.032				E	0.013			E					LOS ANGELES - 16055 VENTURA
461	2	55.0	B	0.040				E	0.023			E					LOS ANGELES - 15910 VENTURA

721223 629 MANAGUA, NICARAGUA

MAG = 6.2

SOIL STATIONS:		***** HORIZONTAL *****											***** VERTICAL *****			STATION LOCATION	
STA#	STRUC	DIST	AC	ACCEL	VEL	DISP	DUR	SRC	ACCEL	VEL	DISP	SRC	ACCEL	VEL	DISP	SRC	
3501	1	5.0	A	0.390				D	0.330			D					MANAGUA, NIC. - ESSO REFINERY

400519 436 IMPERIAL VALLEY, CALIFORNIA

MAG = 6.4

SOIL STATIONS:		***** HORIZONTAL *****											***** VERTICAL *****			STATION LOCATION	
STA#	STRUC	DIST	AC	ACCEL	VEL	DISP	DUR	SRC	ACCEL	VEL	DISP	SRC	ACCEL	VEL	DISP	SRC	
117	1	12.0	B	0.359	36.9	19.8	29.3	A	0.278	10.8	5.6	A					EL CENTRO - IRRIGATION SUBSTA.

ROCK STATIONS:				***** HORIZONTAL *****				***** VERTICAL *****				STATION LOCATION	
STA#	STRUC	DIST	AC	ACCEL	VEL	DISP	DUR	SRC	ACCEL	VEL	DISP		SRC
270	1	105.0	A	0.018				F	0.006			F	PERRIS - RESERVOIR
280	1	122.0	A	0.048	4.2	2.9	0.0	A	0.064	3.7	1.7	A	SAN ONOFRE - SCE NUCLEAR PLANT
116	1	141.0	A	0.011				F	0.009			F	DEVILS CANYON - FILTER PLANT
278	2	168.0	A	0.017				F	0.004			F	SAN DIMAS - PUDDINGSTONE RESERVOIR
104	2	190.0	A	0.004				F	0.001			F	ARCADIA - SANTA ANITA RESERVOIR
266	1	200.0	A	0.007				F	0.002			F	PASADENA - CIT SEISMOLOGY LAB
136	2	203.0	A	0.012	3.1	2.3	0.0	A	0.005	1.2	1.0	A	*LOS ANGELES - SUBWAY TERMINAL
190	2	207.0	A	0.007				F	0.009			F	LOS ANGELES - 2011 ZONAL
279	2	229.0	A	0.009				F	0.006			F	SAN FERNANDO - PACOIMA DAM
121	2	249.0	A	0.003				F	0.001			F	FAIRMONT STATION - RESERVOIR
110	1	256.0	A	0.008				F	0.003			F	CASTAIC - OLD RIDGE ROUTE

SOIL STATIONS:				***** HORIZONTAL *****				***** VERTICAL *****				STATION LOCATION	
STA#	STRUC	DIST	AC	ACCEL	VEL	DISP	DUR	SRC	ACCEL	VEL	DISP		SRC
117	1	45.0	A	0.142	25.8	12.2	3.1	A	0.036	3.4	3.9	A	EL CENTRO - IRRIGATION SUBSTA.
277	2	105.0	A	0.032	6.1	4.4	0.0	A	0.014	1.9	1.3	A	SAN DIEGO - LIGHT & POWER
113	1	130.0	A	0.031	3.5	4.3	0.0	A	0.022	1.8	1.1	A	COLTON - S. CAL. EDISON CO.
274	2	132.0	A	0.018				F	0.003			F	SAN BERNARDINO - HALL OF RECORDS
112	1	147.0	A	0.006				F	0.003			F	CEDAR SPRINGS - PUMP PLANT
281	2	157.0	A	0.013	4.4	3.5	0.0	A	0.006	2.2	1.9	A	SANTA ANA - ORANGE CO. ENG. BLDG
130	1	187.0	A	0.010	3.2	5.0	0.0	A	0.006	1.8	1.8	A	LONG BEACH - TERMINAL ISLAND
131	2	187.0	A	0.005				F	0.003			F	LONG BEACH - UTILITIES BLDG.
288	2	196.0	A	0.019	4.7	2.7	0.0	A	0.008	2.4	1.5	A	VERNON - CENTRAL MFG. TERMINAL
264	2	197.0	A	0.011	2.3	1.8	0.0	A	0.007	1.1	0.8	A	PASADENA - CIT MILLIKAN LIBRARY
475	1	197.0	A	0.010	2.5	2.0	0.0	A	0.004	1.0	1.1	A	PASADENA - CIT ATHENAEUM
181	2	199.0	A	0.013				F	0.003			F	LOS ANGELES - 1640 SOUTH MARENGO
269	1	203.0	A	0.006				F	0.006			F	PEARBLOSSOM - PUMPING PLANT
267	2	204.0	A	0.008	1.3	0.8	0.0	A	0.005	1.0	0.7	A	PASADENA - CIT JPL LAB
122	2	208.0	A	0.023				F	0.017			F	GLENDALE - 633 E. BROADWAY
133	2	211.0	A	0.011				F	0.004			F	*HOLLYWOOD STORAGE - BASEMENT
135	1	211.0	A	0.013	3.2	2.1	0.0	A	0.005	1.1	1.1	A	*HOLLYWOOD STORAGE - P.E. LOT
118	2	227.0	A	0.008				F	0.001			F	LOS ANGELES - 16661 VENTURA
241	2	228.0	A	0.011				F	0.006			F	LOS ANGELES - 8244 ORION
125	1	253.0	A	0.009				F				F	LAKE HUGHES ARRAY 1 - FIRE STATION
2005	2	259.0	A	0.003				F	0.001			F	MOJAVE GENERATING PLANT
1052	1	281.0	A	0.013				F	0.013			F	OSO PUMPING PLANT
272	1	288.0	A	0.003				F				F	PORT HUENEME - NAVY LABORATORY
283	1	341.0	A	0.002				F				F	SANTA BARBARA - COURTHOUSE
1004	1	342.0	A	0.003				F	0.001			F	BAKERSFIELD - HARVEY AUDITORIUM
1095	1	359.0	A	0.002				F				F	TAFT - LINCOLN HS TUNNEL

710209 1400 SAN FERNANDO, CALIFORNIA

MAG = 6.4

ROCK STATIONS:		***** HORIZONTAL *****								***** VERTICAL *****				STATION LOCATION
STA#	STRUC	DIST	AC	ACCEL	VEL	DISP	DUR	SRC	ACCEL	VEL	DISP	SRC		
279	2	3.2	A	1.251	113.2	37.7	13.3	A	0.718	58.3	19.3	A	SAN FERNANDO - PACOIMA DAM	
220	2	16.9	A	0.181	15.0	5.4	6.7	A	0.085	5.0	2.4	A	LOS ANGELES - 3838 LANKERSHIM	
266	1	18.4	A	0.204	11.6	5.0	6.7	A	0.093	5.9	2.3	A	PASADENA - CIT SEISMOLOGY LAB	
141	1	19.4	A	0.188	20.5	7.3	9.6	A	0.138	7.4	3.4	A	LOS ANGELES - GRIFFITH OBSERVATORY	
128	1	21.0	A	0.374	14.6	8.9	14.5	A	0.164	4.1	3.3	A	LAKE HUGHES ARRAY 12 - CWR SITE	
126	1	24.0	A	0.200	8.6	1.7	5.7	A	0.170	7.1	1.6	A	LAKE HUGHES ARRAY 4 - CWR SITE	
127	1	24.0	A	0.147	4.8	2.4	4.6	A	0.089	3.0	2.2	A	LAKE HUGHES ARRAY 9 - CWR SITE	
110	1	26.0	A	0.335	27.8	9.5	19.6	A	0.180	6.4	3.5	A	CASTAIC - OLD RIDGE ROUTE	
104	2	26.0	A	0.223	6.7	5.9	10.9	A	0.070	4.5	2.5	A	ARCADIA - SANTA ANITA RESERVOIR	
190	2	26.6	A	0.083	13.8	10.3	4.2	A	0.060	7.1	3.8	A	LOS ANGELES - 2011 ZONAL	
137	2	27.1	A	0.188	23.4	13.7	6.4	A	0.078	10.3	6.5	A	*LOS ANGELES - WATER & POWER	
121	2	30.0	A	0.103	8.4	1.7	1.8	A	0.043	3.4	1.7	A	FAIRMONT STATION - RESERVOIR	
278	2	47.0	A	0.078	4.6	2.1	1.7	A	0.039	2.3	1.8	A	SAN DIMAS - PUDDINGSTONE RESERVOIR	
290	1	59.0	A	0.057	3.8	1.2	0.1	A	0.037	2.0	1.2	A	WRIGHTWOOD - 6074 PARK DRIVE	
1096	1	64.0	A	0.028	1.4	0.8	0.0	A	0.018	1.0	0.5	A	FORT TEJON - CWR SITE	
1027	1	66.0	A	0.057	2.8	0.9	0.0	A	0.047	2.1	1.2	A	EDMONSTON - GROUND STATION	
111	1	87.0	A	0.021				A	0.010			A	CEDAR SPRINGS - ALLEN RANCH	
282	1	120.0	A	0.019	3.7	2.3	0.0	A	0.011	1.7	1.4	A	GOLETA - UC FLUID MECHANICS LAB	
280	1	121.0	A	0.016	2.8	2.1	0.0	A	0.012	1.5	2.0	A	SAN ONOFRE - SCE NUCLEAR PLANT	

SOIL STATIONS:		***** HORIZONTAL *****								***** VERTICAL *****				STATION LOCATION
STA#	STRUC	DIST	AC	ACCEL	VEL	DISP	DUR	SRC	ACCEL	VEL	DISP	SRC		
241	2	7.7	A	0.258	30.0	14.9	18.7	A	0.178	31.9	14.6	A	LOS ANGELES - 8244 ORION	
458	2	10.7	A	0.118	31.6	17.6	22.7	A	0.111	18.1	7.0	A	LOS ANGELES - 15107 VAN OWEN	
267	2	13.6	A	0.215	13.9	4.9	7.9	A	0.146	5.9	2.6	A	PASADENA - CIT JPL LAB	
461	2	14.8	A	0.148	22.3	8.4	19.5	A	0.120	8.0	2.6	A	LOS ANGELES - 15910 VENTURA	
466	2	15.0	A	0.225	28.3	13.5	18.2	A	0.108	9.4	4.3	A	LOS ANGELES - 15250 VENTURA	
253	2	15.4	A	0.263	31.6	18.3	23.1	A	0.101	9.6	3.8	A	LOS ANGELES - 14724 VENTURA	
122	2	16.5	A	0.273	30.8	11.1	10.2	A	0.142	15.6	5.6	A	GLENDALE - 633 E. BROADWAY	
264	2	21.0	A	0.206	16.4	6.9	10.8	A	0.108	9.0	2.4	A	PASADENA - CIT MILLIKAN LIBRARY	
475	1	22.0	A	0.114	14.3	7.4	8.1	A	0.106	6.6	2.7	A	PASADENA - CIT ATHENAEUM	
482	2	22.6	A	0.121	17.3	8.7	9.1	A	0.084	8.1	3.4	A	ALHAMBRA - 900 SOUTH FREEMONT	
133	2	23.0	A	0.154	19.4	13.1	10.0	A	0.058	6.0	3.8	A	*HOLLYWOOD STORAGE - BASEMENT	
135	1	23.0	A	0.217	21.1	14.7	9.3	A	0.119	5.0	3.0	A	*HOLLYWOOD STORAGE - P.E. LOT	
181	2	26.5	A	0.147	17.6	12.0	10.0	A	0.086	9.0	4.1	A	LOS ANGELES - 1640 SOUTH MARENGO	
125	1	27.0	A	0.152	17.9	3.4	13.1	A	0.102	11.7	2.8	A	LAKE HUGHES ARRAY 1 - FIRE STATION	

262	1	32.0	A	0.150	14.2	3.8	14.5	A	0.105	7.8	2.4	A	PALMDALE - FIRE STATION
288	2	33.0	A	0.111	17.5	14.8	9.1	A	0.047	6.7	4.0	A	VERNON - CENTRAL MFG. TERMINAL
244	2	36.0	A	0.035	11.8	8.8	0.0	A	0.047	6.9	3.9	A	LOS ANGELES - 8639 LINCOLN
247	2	37.0	A	0.045	13.3	10.3	0.0	A	0.025	5.7	3.5	A	LOS ANGELES - 9841 AIRPORT BLVD
229	2	37.0	A	0.069	13.8	9.4	4.6	A	0.028	5.4	3.6	A	LOS ANGELES - 5250 CENTURY BLVD
269	1	41.0	A	0.148	5.4	2.5	10.2	A	0.056	2.3	1.7	A	PEARLBLOSSOM - PUMPING PLANT
1052	1	49.0	A	0.112	8.5	2.3	6.0	A	0.041	3.8	1.2	A	OSO PUMPING PLANT
411	1	54.0	A	0.043	5.0	3.4	0.0	A	0.020	2.2	1.3	A	PALOS VERDES - 2516 VIA TEJON
131	2	58.0	A	0.028	9.6	7.3	0.0	A	0.015	6.1	3.6	A	LONG BEACH - UTILITIES BLDG.
132	2	58.0	A	0.038	9.5	8.0	0.0	A	0.027	4.9	3.8	A	LONG BEACH - STATE COLLEGE
476	2	58.0	A	0.040	5.8	2.7	0.0	A	0.017	2.3	1.9	A	FULLERTON - 2600 NUTWOOD AVE.
130	1	59.0	A	0.030	10.4	8.7	0.0	A	0.016	4.2	2.8	A	LONG BEACH - TERMINAL ISLAND
272	1	62.0	A	0.027	7.3	4.9	0.0	A	0.011	3.2	2.2	A	PORT HUENEME - NAVY LABORATORY
472	2	66.0	A	0.033	8.5	6.5	0.0	A	0.020	3.9	2.5	A	ORANGE - 400 W. CHAPMAN
281	2	70.0	A	0.029	8.0	5.7	0.0	A	0.020	2.4	1.7	A	SANTA ANA - ORANGE CO. ENG. BLDG
114	2	78.0	A	0.036	7.0	6.9	0.0	A	0.010	3.5	2.3	A	COSTA MESA - 666 W. NINETEENTH
1102	1	82.0	A	0.034	2.5	2.1	0.0	A	0.015	2.4	3.3	A	WHFELER RIDGE - GROUND STATION
112	1	88.0	A	0.030				A	0.013			A	CEDAR SPRINGS - PUMP PLANT
113	1	91.0	A	0.039	2.6	1.3	0.0	A	0.026	1.5	1.3	A	COLTON - S. CAL. EDISON CO.
274	2	93.0	A	0.047	3.5	1.3	0.0	A	0.019	1.5	0.8	A	SAN BERNARDINO - HALL OF RECORDS
465	1	104.0	A	0.044	4.6	2.4	0.0	A	0.022	3.4	1.6	A	SAN JUAN CAPISTRANO - CITY HALL
123	1	134.0	A	0.044	2.9	1.7	0.0	A	0.027	2.3	1.3	A	HEMET - FIRE STATION
103	1	168.0	A	0.037	2.6	1.2	0.0	A	0.015	1.4	1.1	A	ANZA - ANZA POST OFFICE

39

490413 1955 PUGET SOUND, WASHINGTON

MAG = 7.1

SOIL STATIONS:		***** HORIZONTAL *****							***** VERTICAL *****				STATION LOCATION
STA#	STRUC	DIST	AC	ACCEL	VEL	DISP	DUR	SRC	ACCEL	VEL	DISP	SRC	
2101	1	48.0	C	0.306	21.4	10.4	22.3	A	0.111	7.0	4.0	A	OLYMPIA - HIGHWAY TEST LAB
2170	1	69.0	C	0.072	8.2	2.7	14.8	A	0.024	2.4	2.3	A	SEATTLE ARMY BASE - 4735 E MARGINAL

590818 637 HEBGEN LAKE, MONTANA

MAG = 7.1

ROCK STATIONS:		***** HORIZONTAL *****							***** VERTICAL *****				STATION LOCATION
STA#	STRUC	DIST	AC	ACCEL	VEL	DISP	DUR	SRC	ACCEL	VEL	DISP	SRC	
2201	1	175.0	C	0.043				R	0.021			B	BUTTE, MONT. - SCHOOL OF MINES
2202	2	208.0	C	0.013				R	0.008			B	HELENA, MONT. - CARROL COLLEGE
2204	1	454.0	C	0.001				R	0.001			B	HUNGRY HORSE - DOWNSTREAM STATION

SOIL STATIONS:		***** HORIZONTAL *****							***** VERTICAL *****				STATION LOCATION
STA#	STRUC	DIST	AC	ACCEL	VEL	DISP	DUR	SRC	ACCEL	VEL	DISP	SRC	
2205	2	95.0	C	0.055				B	0.026			B	BOZEMAN, MONT. - STATE COLLEGE

520721 1152 KERN COUNTY, CALIFORNIA

MAG = 7.2

ROCK STATIONS:		***** HORIZONTAL *****							***** VERTICAL *****				STATION LOCATION
STA#	STRUC	DIST	AC	ACCEL	VEL	DISP	DUR	SRC	ACCEL	VEL	DISP	SRC	
136	2	115.0	B	0.032				B	0.008			B	*LOS ANGELES - SUBWAY TERMINAL
1083	1	148.0	B	0.014				R	0.009			B	SAN LUIS OBISPO - CITY REC. BLDG

SOIL STATIONS:		***** HORIZONTAL *****							***** VERTICAL *****				STATION LOCATION
STA#	STRUC	DIST	AC	ACCEL	VEL	DISP	DUR	SRC	ACCEL	VEL	DISP	SRC	
1095	1	42.0	B	0.196	17.7	9.1	19.6	A	0.123	6.7	5.0	A	TAFT - LINCOLN HS TUNNEL
283	1	85.0	B	0.135	19.3	5.8	13.8	A	0.051	5.0	2.1	A	SANTA BARBARA - COURTHOUSE
133	2	107.0	B	0.058	9.4	5.9	0.1	A	0.024	4.2	2.2	A	*HOLLYWOOD STORAGE - BASEMENT
135	1	107.0	B	0.062	8.9	6.4	0.1	A	0.022	3.1	3.4	A	*HOLLYWOOD STORAGE - P.E. LOT
475	1	109.0	B	0.054	9.1	2.9	0.1	A	0.033	4.5	3.0	A	PASADENA - CIT ATHENAEUM
288	2	122.0	B	0.037				R	0.012			B	VERNON - CENTRAL MFG. TERMINAL
131	2	145.0	B	0.016				R	0.006			B	LONG BEACH - UTILITIES BLDG.
113	1	156.0	B	0.014				B	0.012			B	COLTON - S. CAL. EDISON CO.
1008	1	224.0	B	0.018				B	0.006			B	BISHOP - LA WATER DEPT GARAGE
277	2	282.0	B	0.005				R	0.001			B	SAN DIEGO - LIGHT & POWER
1028	1	293.0	B	0.010				B	0.005			B	HOLLISTER - CITY HALL
2001	1	359.0	B	0.004				R					HAWTHORNE - US NAVY AMMO. DEPOT
1081	2	366.0	B	0.004				R					SAN JOSE - BANK OF AMERICA BLDG
117	1	370.0	B	0.004				R	0.003			B	EL CENTRO - IRRIGATION SUBSTA.
1049	2	407.0	B	0.001				R					OAKLAND - CITY HALL
1078	2	425.0	B	0.004				B					SAN FRANCISCO - SOUTHERN PACIFIC BG

40

720730 2145 SITKA, ALASKA

MAG = 7.6

ROCK STATIONS:		***** HORIZONTAL *****							***** VERTICAL *****				STATION LOCATION
STA#	STRUC	DIST	AC	ACCEL	VEL	DISP	DUR	SRC	ACCEL	VEL	DISP	SRC	
2714	1	45.0	B	0.110				R	0.050			B	SITKA, ALASKA - MAGNETIC OBS.
2708	1	145.0	B	0.010				R					JUNEAU, AUKE BAY - BUR OF COMM FISH

SOIL STATIONS:		***** HORIZONTAL *****							***** VERTICAL *****				STATION LOCATION
STA#	STRUC	DIST	AC	ACCEL	VEL	DISP	DUR	SRC	ACCEL	VFL	DISP	SRC	
2715	1	300.0	B	0.010				B					YAKUTAT, ALASKA - AIRPORT PUMP HOUSE

SOURCES OF STRONG MOTION DATA

CODE REFERENCE

A EARTHQUAKE ENGINEERING RESEARCH LABORATORY (1969-1975)
 B U.S. DEPT. OF COMMERCE (SERIAL PUBLICATION)
 C CLOUD AND KNUDSON (NO DATE)
 D U. S. GEOLOGICAL SURVEY (1974)
 E A. G. BRADY (U. S. GEOLOGICAL SURVEY, WRITTEN COMMUN., 1977)
 F U. S. COAST AND GEODETIC SURVEY AND EARTHQUAKE ENGINEERING RESEARCH LABORATORY (1968)
 G U. S. GEOLOGICAL SURVEY (1975)
 H MALEY AND OTHERS (1975)
 I U. S. GEOLOGICAL SURVEY (1976A)

LISTING OF STATIONS

STA#	STRUC	GEO	LOCATION	STRUCTURE	REF	GEOLOGY	REF
103	1	S	ANZA - ANZA POST OFFICE	1 STORY BLDG	1	ALLUVIUM	2
104	2	R	ARCADIA - SANTA ANITA RESERVOIR	ABUTMENT, C DAM	1	GRANITE/DIORITE	2
110	1	R	CASTAIC - OLD RIDGE ROUTE	INST SHELTER	1	SANDSTONE	1
111	1	R	CEDAR SPRINGS - ALLEN RANCH	1 STORY BLDG	1	GRANITIC	2
112	1	S	CEDAR SPRINGS - PUMP PLANT	1 STORY BLDG	1	SHALLOW ALLUVIUM	2
113	1	S	COLTON - S. CAL. EDISON CO.	1 STORY BLDG	1	DEEP ALLUVIUM	1
114	2	S	COSTA MESA - 666 W. NINETEENTH	18 STORY BLDG	1	ALLUVIUM	1
116	1	R	DEVILS CANYON - FILTER PLANT	1 STORY BLDG	1	LS/GNEISS	2
117	1	S	EL CENTRO - IRRIGATION SUBSTA.	2 STORY BLDG	1	>300 M ALLUVIUM	1
118	2	S	LOS ANGELES - 16661 VENTURA	8 STORY RC BLDG	1	8M ALLUV/SHALE	1
121	2	R	FAIRMONT STATION - RESERVOIR	ABUTMENT, E DAM	1	GRANITE	1
122	2	S	GLENDALE - 633 E. BROADWAY	3 STORY BLDG	1	>8 M ALLUVIUM	1
123	1	S	HEMET - FIRE STATION	1 STORY BLDG	1	ALLUVIUM	1
125	1	S	LAKE HUGHES ARRAY 1 - FIRE STATION	1 STORY BLDG	1	300 M ALLUVIUM	1
126	1	R	LAKE HUGHES ARRAY 4 - CWR SITE	INST SHELTER	1	WEATHERED GRANIT	1
127	1	R	LAKE HUGHES ARRAY 9 - CWR SITE	1 STORY BLDG	1	GNEISS	1
128	1	R	LAKE HUGHES ARRAY 12 - CWR SITE	1 STORY BLDG	1	THIN ALLUVIUM	1
129	2	S	LOMA LINDA - UNIV. MED. CENTER	10 STORY BLDG	3	APP 250 M ALLUV	3
130	1	S	LONG BEACH - TERMINAL ISLAND	1 STORY BLDG	1	DEEP ALLUVIUM	1
131	2	S	LONG BEACH - UTILITIES BLDG.	4 STORY BLDG	1	DEEP ALLUVIUM	1
132	2	S	LONG BEACH - STATE COLLEGE	9 STORY BLDG	1	>15 M ALLUVIUM	1
133	2	S	* HOLLYWOOD STORAGE - BASEMENT	14 STORY RC	1	130 M ALLUVIUM	1
135	1	S	* HOLLYWOOD STORAGE - P.E. LOT	INST SHELTER	1	130 M ALLUVIUM	1
136	2	R	* LOS ANGELES - SUBWAY TERMINAL	12 STORY BLDG	3	120 M SHALE	3
137	2	R	* LOS ANGELES - WATER & POWER	15 STORY STEEL	1	MIOCENE SILTSTNE	2
141	1	R	LOS ANGELES - GRIFFITH OBSERVATORY	INST SHELTER	1	GRANITE	1
181	2	S	LOS ANGELES - 1640 SOUTH MARENGO	7 STORY RC	1	>16 M ALLUVIUM	1
190	2	R	LOS ANGELES - 2011 ZONAL	9 STORY RC	1	ALLUVIUM 0-10 M	1
220	2	R	LOS ANGELES - 3838 LANKERSHIM	20 STORY RC	1	SH & SS	1
229	2	S	LOS ANGELES - 5250 CENTURY BLVD	7 STORY STEEL	1	>16 M ALLUVIUM	1
241	2	S	LOS ANGELES - 8244 ORION	7 STORY RC	1	>13 M ALLUVIUM	1
244	2	S	LOS ANGELES - 8639 LINCOLN	12 STORY RC	1	>18 M ALLUVIUM	1
247	2	S	LOS ANGELES - 9841 AIRPORT BLVD	14 STORY RC	1	>23 M ALLUVIUM	1
253	2	S	LOS ANGELES - 14724 VENTURA	12 STORY RC	1	>24 M ALLUVIUM	1
259	2	S	LOS ANGELES - 16055 VENTURA	12 STORY BLDG	1	12M ALLUV/SHALE	1
262	1	S	PALMDALE - FIRE STATION	1 STORY BLDG	1	ALLUVIUM	2
264	2	S	PASADENA - CIT MILLIKAN LIBRARY	9 STORY RC	1	APP 300 M ALLUV	2
266	1	R	PASADENA - CIT SEISMOLOGY LAB	2 STORY BLDG	1	GRANITE	1
267	2	S	PASADENA - CIT JPL LAB	9 STORY STEEL	1	SANDY GRAVEL	2
269	1	S	PEARBLOSSOM - PUMPING PLANT	INST SHELTER	1	130 M ALLUVIUM	2
270	1	R	PERRIS - RESERVOIR	INST SHELTER	1	ALLUV VEN/GRANIT	2
272	1	S	PORT HUENEME - NAVY LABORATORY	1 STORY WAREHSE	1	>300 M ALLUVIUM	1
277	2	S	SAN DIEGO - LIGHT & POWER	4 STORY BLDG	1	DEEP ALLUVIUM	1
274	2	S	SAN BERNARDINO - HALL OF RECORDS	6 STORY BLDG	1	>35 M ALLUVIUM	1
278	2	R	SAN DIMAS - PUDDINGSTONE RESERVOIR	ABUTMENT-EARTH	1	VOL CLASTICS-SH	2
279	2	R	SAN FERNANDO - PACOIMA DAM	ABUTMENT-CONCRET	1	JOINTED GNEISS	2
280	1	R	SAN ONOFRE - SCE NUCLEAR PLANT	1 STORY WAREHSE	1	SOFT SANDSTONE	1
281	2	S	SANTA ANA - ORANGE CO. ENG. BLDG	3 STORY BLDG	1	ALLUVIUM	1
282	1	R	GOLETA - UC FLUID MECHANICS LAB	1 STORY BLDG	1	4 M ALLUV/SILTST	1
283	1	S	SANTA BARBARA - COURTHOUSE	2 STORY BLDG	1	>10 M ALLUVIUM	1

288	2	S	VERNON - CENTRAL MFG. TERMINAL	6 STORY BLDG	1	DEEP ALLUVIUM	1
290	1	R	WRIGHTWOOD - 6074 PARK DRIVE	2 STORY BLDG	1	ALLUV VEN/IGN	2
319	2	S *	LOS ANGELES - UCLA ENGINEERING BLDG	4 STORY BLDG	3	21 M ALLUVIUM	3
411	1	S	PALOS VERDES - 2516 VIA TEJON	2 STORY BLDG	1	SHALLOW SANDS/SH	2
458	2	S	LOS ANGELES - 15107 VAN OWEN	7 STORY RC	1	>23 M ALLUVIUM	1
461	2	S	LOS ANGELES - 15910 VENTURA	18 STORY STEEL	1	>12 M ALLUVIUM	1
465	1	S	SAN JUAN CAPISTRANO - CITY HALL	1 STORY BLDG	1	ALLUVIUM	2
466	2	S	LOS ANGELES - 15250 VENTURA	12 STORY RC	1	>12 M ALLUVIUM	1
472	2	S	ORANGE - 400 W. CHAPMAN	19 STORY BLDG	1	>100 M ALL/SHALE	2
475	1	S	PASADENA - CIT ATHENAEUM	2 STORY RC	3	APPROX 200 M ALL	3
476	2	S	FULLERTON - 2600 NUTWOOD AVE.	10 STORY RC	1	>20 M ALLUVIUM	1
482	2	S	ALHAMBRA - 900 SOUTH FREEMONT	12 STORY STEEL	1	APPROX 100 M ALL	2
497	2	S	LOS ANGELES - 16633 VENTURA	14 STORY BLDG	1	ALLUVIUM	1
512	2	S	LOS ANGELES - 16255 VENTURA	12 STORY BLDG	1	20M ALLUV/SHALE	1
610	2	S	LOS ANGELES - 18321 VENTURA	10 STORY BLDG	1	>5M ALLUVIUM	1
655	1	R	JENSEN FILTER PLT - 13100 BALBOA, LA	2 STORY BLDG	1	ROCK	7
657	2	S	SANTA MONICA - 201 OCEAN	18 STORY BLDG	1	SOIL	7
1001	1	S	APEEL ARRAY - STATION 1	INST SHELTER	1	210M ALLUVIUM	1
1002	1	S	APEEL ARRAY - STATION 2	INST SHELTER	1	8M MUD/85M ALLUV	1
1004	1	S	BAKERSFIELD - HARVEY AUDITORIUM	AUDITORIUM	1	>250 M ALLUVIUM	1
1008	1	S	BISHOP - LA WATER DEPT GARAGE	1 STORY BLDG	3	200 M ALLUVIUM	3
1011	1	S	BUENA VISTA - GROUND STATION	INST SHELTER	1	ALLUVIUM	2
1013	1	S	CHOLAME-SHANDON ARRAY NO. 2	INST SHELTER	1	45 M ALLUV/SS	1
1014	1	S	CHOLAME-SHANDON ARRAY NO. 5	INST SHELTER	1	ALLUVIUM	1
1015	1	S	CHOLAME-SHANDON ARRAY NO. 8	1 STORY BLDG	1	THIN ALLUVIUM/SS	1
1016	1	S	CHOLAME-SHANDON ARRAY NO. 12	INST SHELTER	1	30 M TERRACE/SS	1
1023	1	S	FERNDALE - OLD CITY HALL, BROWN ST	2 STORY BLDG	1	ALLUVIUM	1
1027	1	R	EDMONSTON - GROUND STATION	INST SHELTER	1	5 M ALLUV/GNEISS	2
1028	1	S	HOLLISTER - CITY HALL	1 STORY BLDG	3	13 M ALLUVIUM	3
1032	1	R	SAGO CENTRAL - HARRIS RANCH	INST SHELTER	1	ROCK	6
1049	2	S	OAKLAND - CITY HALL	15 STORY BLDG	3	76 M MUD-ALLUVIUM	3
1051	1	R	OROVILLE SEISMOGRAPH STATION	1 STORY BLDG	1	METAVOLCANICS	1
1052	1	S	OSO PUMPING PLANT	INST SHELTER	1	ALLUVIUM	2
1057	1	R	PLEASANT HILL - DIABLO VALLEY COL.	2 STORY BLDG	3	2 M ALUV/SS	3
1065	2	S	SAN FRANCISCO - ALEXANDER BLDG	15 STORY BLDG	3	46 M ALLUVIUM	3
1071	2	S	SAN FRANCISCO - BETHLEHEM PAC BLDG	14 STORY BLDG	1	70M ALLUVIUM	1
1074	2	R	SAN FRANCISCO - 390 MAIN	7 STORY BLDG	1	SHALE/SS	1
1078	2	S	SAN FRANCISCO - SOUTHERN PACIFIC BG	12 STORY BLDG	3	90 M FILL-ALLUV	3
1080	2	S	SAN FRANCISCO - STATE BLDG	7 STORY BLDG	3	61 M ALLUVIUM	3
1081	2	S	SAN JOSE - BANK OF AMERICA BLDG	13 STORY BLDG	3	APPROX 750 M ALL	3
1083	1	R	SAN LUIS OBISPO - CITY REC. BLDG	2 STORY BLDG	1	2 M LOAM/FRAN SH	2
1093	1	S	SAN PABLO - CONTRA COSTA COLLEGE	2 STORY BLDG	3	6 M FILL-ALLUV	3
1095	1	S	TAFT - LINCOLN HS TUNNEL	1 STORY SCH BLDG	1	ALLUVIUM	1
1096	1	R	FORT TEJON - CWR SITE	1 STORY BLDG	1	GRANITE	1
1102	1	S	WHEELER RIDGE - GROUND STATION	INST SHELTER	1	APPROX 100 M ALL	2
1117	1	R	SAN FRANCISCO - GOLDEN GATE PARK	INST SHELTER	3	FRAN CHERT-SHALE	3
1202	1	S	STONE CANYON EAST, CALIF.	1 STORY BLDG	1	SOIL	8
1249	1	R	CAPE MENDOCINO (C5) - PETROLIA	INST SHELTER	1	CRETACEOUS ROCK	1
1250	1	S	GILROY (C6) - GEOL BLDG, GAL COL	1 STORY BLDG	1	TERRACE DEPOSITS	1
1278	1	R	SHELTER COVE, STA 2 (C41) - PWR PLT	INST SHELTER	1	FRANCISCAN ROCK	1
1291	1	S	MARYSVILLE (C56) - CDOT MAINT BLDG	1 STORY BLDG	1	100M ALLUVIUM	1
1292	1	S	CHICO (C57) - 2334 FAIR STREET	1STORY BLDG	1	90M ALLUVIUM	1
1293	1	R	PARADISE (C58) - KEWG TRNSMTR BLDG	1 STORY BLDG	1	VOLCANIC ROCK	1
1377	1	S	SAN JUAN BAUTISTA (C126) - 24 POLK	1 STORY BLDG	1	SOIL	6
1398	1	S	PETROLIA (C156) - GENERAL STORE	INST SHELTER	1	ALLUVIUM	1

1438	1	R	CHOLAME-SHANDON; TEMBLOR	INST SHELTER	1	ROCK	9
2001	1	S	HAWTHORNE - US NAVY AMMO. DEPOT	1 STORY BLDG	1	ALLUVIUM	1
2005	2	S	MOJAVE GENERATING PLANT	LRG POWER PLANT	3	APPROX 70 M ALLU	3
2101	1	S	OLYMPIA - HIGHWAY TEST LAB	INST SHELTER	1	ALLUVIUM	5
2170	1	S	SEATTLE ARMY BASE - 4735 E MARGINAL	1 STORY BLDG	1	ALLUVIUM	5
2201	1	R	BUTTE, MONT. - SCHOOL OF MINES	2 STORY BLDG	3	GRANITIC INTRUS	3
2202	2	R	HELENA, MONT. - CARROL COLLEGE	5 STORY BLDG	3	GRANITICS	3
2204	1	R	HUNGRY HORSE - DOWNSTREAM STATION	INST SHELTER	3	LIMESTONE	3
2205	2	S	BOZEMAN, MONT. - STATE COLLEGE	3 STORY BLDG	3	APPROX 170 M ALL	3
2707	1	R	FAIRBANKS, ALASKA - UNIV OF ALASKA	INST SHELTER	3	SCHIST	3
2708	1	R	JUNEAU, AUKE BAY - BUR OF COMM FISH	1 STORY BLDG	1	SLATE	1
2714	1	R	SITKA, ALASKA - MAGNETIC OBS.	INST SHELTER	1	GRAYWACKE	1
2715	1	S	YAKUTAT, ALASKA - AIRPORT PUMP HOUSE	1 STORY BLDG	1	GLACIAL OUTWASH	1
3501	1	S	MANAGUA, NIC. - ESSO REFINERY	1 STORY BLDG	4	ALLUVIUM	4

REFERENCE LISTING

CODE REFERENCE

- 1 U. S. GEOLOGICAL SURVEY (1976B)
- 2 MALEY AND CLOUD (1973)
- 3 R. P. MALEY (U. S. GEOLOGICAL SURVEY, WRITTEN COMMUN., 1975)
- 4 VALERA (1973)
- 5 TRIFUNAC AND BRADY (1975)
- 6 JENNINGS AND STRAND (1959)
- 7 JENNINGS AND STRAND (1969)
- 8 R. P. MALEY (U. S. GEOLOGICAL SURVEY, ORAL COMMUN., 1977)
- 9 CLOUD AND PEREZ (1967)

